Short title: AtBAG4 is a KAT1 potassium channel regulator

**Author for Contact details*
Lynne Yenush
Instituto de Biología Molecular y Celular de Plantas, Universitat Politécnica de Valencia-Consejo Superior de Investigaciones Científicas, 46022 Valencia, SPAIN
+34963879375

Title: BCL2-ASSOCIATED ATHANOGENE4 Regulates the KAT1 Potassium Channel and Controls Stomatal Movement

Author names and affiliations: Antonella Locascio[1], Mª Carmen Marqués[1], Guillermo García-Martínez[1], Claire Corratgé-Faillie[2], Nuria Andrés-Colás[1], Lourdes Rubio[3], José Antonio Fernández[3], Anne-Aliénor Véry[2], José Miguel Mulet[1], Lynne Yenush[1*]

[1] *Instituto de Biología Molecular y Celular de Plantas, Universitat Politécnica de Valencia-Consejo Superior de Investigaciones Científicas, 46022 Valencia, SPAIN*

[2] *Biochimie et Physiologie Moléculaire des Plantes, Univ Montpellier, CNRS, INRA, SupAgro Montpellier, Campus SupAgro-INRA, 34060 Montpellier Cedex 2, France*

[3] *Facultad de Ciencias.Universidad de Málaga.Campus de Teatinos S/N 29010 Málaga, SPAIN*

One Sentence summary: The evolutionarily conserved Arabidopsis protein BAG4 regulates the KAT1 potassium channel and stomatal movement, and is a possible target for development of plants with increased water use efficiency.

Author Contributions: AL, MM, GG-M, NA-C, CC-F and LY performed the experiments; LY and JMM designed and supervised the project; LY, JMM, AL, LR, A-AV, JAF and CC-F participated in the experimental design and writing of the manuscript.

Funding Information: This work was supported by the Spanish Ministry of Economy and Competitiveness (BIO201677776-P and BIO2016-81957-REDT) and the Valencian Government (AICO/2018/300).

Email address for Author for Contact: *lynne@ibmcp.upv.es*

Abstract

Potassium (K^+) is a key monovalent cation necessary for multiple aspects of cell growth and survival. In plants, this cation also plays a key role in the control of stomatal movement. KAT1 and its homolog KAT2 are the main inward rectifying channels present in guard cells, mediating K^+ influx into these cells, resulting in stomatal opening. To gain further insight into the regulation of these channels, we performed a split-ubiquitin protein-protein interaction screen searching for KAT1 interactors in Arabidopsis (*Arabidopsis thaliana*). We characterized one of these candidates, BCL2-ASSOCIATED ATHANOGENE4 (BAG4), in detail using biochemical and genetic approaches to confirm this interaction and its effect on KAT1 activity. We show that BAG4 improves KAT1-mediated K^+ transport in two heterologous systems and provide evidence that in plants, BAG4 interacts with KAT1 and favors the arrival of KAT1 at the plasma membrane. Importantly, lines lacking or overexpressing the *BAG4* gene show altered KAT1 plasma membrane accumulation and alterations in stomatal movement. Our data allowed us to identify a KAT1 regulator and define a potential target for the plant BAG family. The identification of physiologically relevant regulators of K^+ channels will aid in the design of approaches that may impact drought tolerance and pathogen susceptibility.

Key words: Arabidopsis, BAG4, K^+ channel regulator, KAT1, KAT2, stomata regulation

Introduction

Ion homeostasis is a dynamic process essential for the normal functioning of any organism. Some minerals are required for biological processes, but their excess or deficiency is deleterious. In addition, cells must discriminate between the physiologically relevant ions and the toxic ions that may be chemically similar. For this reason, all living organisms have developed efficient systems to capture and store ions and complex mechanisms to maintain homeostatic concentrations. In plants, ion homeostasis must provide the environment required to maintain all internal processes, prevent toxicity and enable the response to environmental changes using the minerals present in the soil.

Potassium is a key monovalent cation necessary for many aspects of growth and survival, among them, compensation of the negative charges generated in processes such as glycolysis, the maintenance of electroneutrality, turgor pressure and cell volume, phloem loading, enzymatic activity, protein synthesis and the establishment of proper membrane potential and an adequate intracellular pH (Rodríguez-Navarro, 2000).

In plant cells, potassium accumulates to relatively high concentrations in the plant cell cytosol (about 100 mM) and in variable amounts in the vacuole (10-200 mM, depending on the tissue and the environmental conditions), while other cations such as sodium must be excluded to avoid toxicity (Pardo and Quintero, 2002). Potassium homeostasis is essential for optimal water use efficiency, as potassium currents participate in stomatal movement. Stomatal opening depends on potassium and anion uptake coupled to increased proton efflux, while stomatal closing depends on potassium and anion efflux (Lawson and Blatt, 2014). Understanding the molecular mechanisms underlying potassium regulation in guard cells can provide valuable information with applications to the development of new varieties of drought resistant crops. In response to elevated CO_2, drought may be among the main threats to world food production because of its dramatic impact on agricultural productivity. Optimizing water use efficiency of crops by improving the potassium regulation in the guard cell, and

therefore improving transpiration regulation, can directly affect food production under adverse conditions (Wang et al., 2014).

In the model plant *Arabidopsis thaliana*, there are three different families of plasma membrane potassium transport systems: the CPA2 subfamily including CHX and KEA H^+/K^+ antiporters (Mäser et al., 2001), the HAK/KUP/KT K^+ transporters (Gierth and Mäser, 2007), and the Shaker-type K^+ channels (Véry and Sentenac, 2003). The third family, Shaker channels, is present in animals, plants, yeast and bacteria. The genome of Arabidopsis contains 9 members that are classified into 5 different groups depending on their phylogeny and functional aspects (Pilot et al., 2003). Groups 1 and 2 contain 4 inward rectifying channels (AKT1, AKT6, KAT1 and KAT2, respectively), while group 3 contains a weak inward rectifier (AKT2). Group 4 contains a "Silent" channel (KC1) and group 5 consists of two outwardly rectifying channels (GORK and SKOR). This family of voltage-dependent channels selective for potassium is responsible for the K^+ conductance in the plasma membrane in most cell types. Based on the structural data obtained for bacterial and mammalian Shaker channels, it has been proposed that this family adopts a homo- or hetero-tetrameric structure that forms the potassium pore (Jiang et al., 2003; Long et al., 2005). For example, AKT1 has been proposed to form functional channels with KC1 and KAT2, while KAT1 and KAT2 can associate with each other and also with KC1 (and AKT2 in the case of KAT2) (Lebaudy et al., 2010; Jeanguenin et al., 2011). KC1 is considered a "silent" channel since it is only able to induce currents when it is part of heterotetramers (Dreyer et al., 1997; Duby et al., 2008; Jeanguenin et al., 2011). It is considered that this multiplicity in the composition of subunits confers different properties to the channel and this would be a reflection of different physiological functions (Ivashikina et al., 2001; Xicluna et al., 2007; Jeanguenin et al., 2011).

Two members of the Shaker family, KAT1 and KAT2 are major contributors to potassium influxes in guard cells (Nakamura et al., 1995; Szyroki et al., 2001; Lebaudy et al., 2008). As potassium homeostasis contributes to the regulation of stomatal movement, this process requires tight regulation, which allows fast activation and inactivation, to prevent excessive water loss, specifically under drought or saline conditions (Lebaudy et al., 2008). Therefore, the identification and characterization of the proteins interacting

with the KAT1 potassium channel may provide new insights into potassium homeostasis regulation and new ways to develop drought tolerant plants.

KAT1 is considered the prototype of inward rectifying potassium channels and plays an important role in potassium fluxes in the guard cell, as mentioned above (Anderson et al., 1992; Schachtman et al., 1992; Nakamura et al., 1995). Several proteins have been implicated in KAT1 regulation. For example, it has been described that fusicoccin can stabilize the interaction of KAT1 with 14-3-3 proteins and activate its transport activity (Saponaro et al., 2017), but the underlying mechanism of this regulation at the level of protein-protein interaction remains largely unexplored. Previous studies have shown that both the Ost1 (SnRK2.6) and the CPK13 kinases can phosphorylate KAT1, although the molecular mechanism by which these phosphorylation events regulate the channel are as yet undefined (Sato et al., 2009; Ronzier et al., 2014). In addition, work from the Blatt laboratory has shown that VAMP721 and SYP121 are important for KAT1 trafficking and gating of the channel (Sutter et al., 2006; Eisenach et al., 2012; Zhang et al., 2015; Zhang et al., 2017; Lefoulon et al., 2018). As these channels play an instrumental role in stomatal movement, their regulation is likely to be complex, involving several different classes of regulatory molecules.

In the present report, we used a split-ubiquitin approach to identify proteins interacting with KAT1. We found that the BCL2-Associated Athanogene (BAG) 4 protein interacts with KAT1. BAG4 is a member of an evolutionarily conserved family defined by the presence of the BAG domain. This domain is approximately 110-125 amino acids long and is composed of three antiparallel α helices of 30-40 amino acids (Takayama and Reed, 2001). BAG family proteins have been extensively studied in mammalian systems where they have been shown to regulate several processes in many cases by recruiting co-chaperones and different chaperone systems, including the Heat shock protein 70 (Hsp70), which binds to helices 2 and 3 of the BAG domain (Takayama and Reed, 2001; Kabbage and Dickman, 2008). In plants, BAG proteins have been related to processes such as the unfolded protein response, pathogen resistance and abiotic stress and have been shown to conserve the ability to bind to Hsp70 (Doukhanina et al., 2006; Williams et al., 2010; Kabbage et al., 2016), although the molecular mechanisms underlying their function are largely undefined. More specifically, overexpression of BAG4 is able to

increase salinity tolerance in Arabidopsis and rice (Doukhanina et al., 2006; Hoang et al., 2015), and BAG1 and BAG6 have been implicated in the proteasomal degradation of plastid proteins and fungal resistance, respectively (Kabbage et al., 2016; Lee et al., 2016). In this report, we show that BAG4 expression increases KAT1 activity in both yeast and *Xenopus* oocytes. Moreover, we have confirmed the KAT1-BAG4 interaction in plants and provide evidence that BAG4 plays a role in the arrival of KAT1 at the plasma membrane in both gain- and loss-of-function experiments. In addition, mutants lacking or overexpressing the *BAG4* gene present alterations in stomatal opening dynamics, consistent with a physiological role in modulating potassium fluxes. Taken together, our data suggest that in plants BAG4 acts as a KAT1 regulator. Our work uncovers an important potential client for the plant BAG protein family.

Results

In order to gain further insight into the post-translational regulation of the KAT1 inward rectifying potassium channel, we carried out a high-throughput screening for physical interactors using the Split-ubiquitin yeast two-hybrid assay with an Arabidopsis cDNA library, as described in Materials and Methods. Previous reports have shown that KAT1 interactions can be detected using this method (Obrdlik et al., 2004). Using this approach, we identified BAG4 as a KAT1 interacting protein.

As a first step in the characterization of this interaction, we carried out a functional complementation assay in yeast for selected candidates. We co-transformed KAT1 with BAG4 and two other candidate proteins into a yeast strain lacking its endogenous high affinity potassium transporters (Trk1 and Trk2). This strain grows very poorly in media with limiting amounts of potassium (12 µM) (Navarrete et al., 2010). However, KAT1 expression functionally complements this phenotype. The plasmid containing the *KAT1* sequence is under control of the *MET25* promoter and in the presence of 0.75 mg/ml methionine the expression of *KAT1* is reduced to low levels (Mumberg et al., 1994), providing a sensitive system to study KAT1 activity. In order to determine whether BAG4 could functionally regulate KAT1, we performed growth assays in liquid media under three conditions: 1) low KAT1 expression (methionine supplementation) and low potassium (no KCl supplementation), 2) low KAT1 expression and high potassium (50 mM KCl), and 3) high KAT1 expression and low potassium. As shown in Fig. 1, co-expression of BAG4 with KAT1 improved growth under limiting potassium conditions, whereas two other Arabidopsis proteins recovered in the screening, (PPI1 (Proton pump interacting protein 1) and RPT2 (Root phototropism 2)), had no functional effect in this assay. Correct expression of the proteins was confirmed by immunodetection (Fig. 1). As observed, both BAG4 and PPI1 accumulated to similar levels, whereas RPT2 accumulated to lower levels in yeast. This result is consistent with BAG4 improving KAT1 activity in this heterologous system. Based on this phenotype, BAG4 was selected for further analysis. We next wanted to confirm that the increase in growth in this assay was not due to increased expression of the KAT1 protein upon BAG4 overexpression. For this, we determined the levels of KAT1 in 6 control strains and 7 strains co-expressing BAG4. As shown in Figure 1, we observed no change in KAT1 protein levels, suggesting

that the effect of BAG4 is not due to increased accumulation of KAT1, and so discards mechanisms based on transcriptional regulation and protein turnover in this model system.

BAG4 belongs to a seven member family of proteins all containing a BAG domain (Doukhanina et al., 2006). BAG1 and BAG7 have a domain structure similar to BAG4 and so were chosen for further analysis. Using the yeast assays described above, we compared both the interaction and the functional complementation between BAG family members. Since the original BAG4 clone recovered from the screening had a 13 amino acid N-terminal truncation, we cloned the full-length *BAG4* gene and included it in these assays. As observed in the split-ubiquitin protein-protein interaction assay shown in Figure 2, we observed the strongest interaction between KAT1 and the BAG4 isoforms, as judged by the growth in selective media and the X-gal plate assay. A moderate interaction was observed for BAG1, whereas the interaction between KAT1 and BAG7 was very weak. The data presented in Figure 2 confirms the proper expression of each of the proteins. The same pattern of relative KAT1-BAG protein interaction (BAG4>BAG1>>BAG7) was observed in the functional complementation assay shown in Figure 2. The combinations between KAT1 and both versions of BAG4 show the highest growth in low potassium medium when KAT1 is limiting (black bars). Some growth is detected under these conditions upon co-expression of BAG1, but in the presence of BAG7 the level of growth is the same as the control. Thus, we provide evidence for some level of specificity between KAT1 and BAG family members, lending further support to the possible physiological relevance of the KAT1-BAG4 interaction.

In order to confirm that the observed improvement in growth of the KAT1_BAG4 strain is due to improved potassium uptake, we analyzed potassium uptake using K^+-specific electrodes (see Materials and Methods for a complete description). As shown in Figure 3, co-expression of BAG4 increased both the total amount and the initial rate of potassium uptake from the media. As an internal control, we measured the acidification of the media (due to the H^+-ATPase activity) and, as expected, observed no changes in the presence or absence of BAG4 (Fig. 3). These experiments strongly suggest that BAG4 favors KAT1 potassium transport activity, at least in yeast.

Xenopus oocytes have been extensively used to characterize potassium channels from many organisms. We studied the effect of BAG4 co-expression on KAT1-mediated currents in this model system. We observed an increase in KAT1 channel activity one day after cRNA injection into the oocytes (Fig. 4 and Supplemental Fig. S1). At later times (from Day 2), when reaching steady-state expression level, no differences in the currents were observed (Supplemental Fig. S1). KAT1 current increase upon BAG4 co-expression one day after oocyte injection was 50% to 100% in the different experiments at all membrane voltages (Fig. 4 and Supplemental Fig. S1). No shift in KAT1 voltage-dependence was observed under co-expression (Fig. 4). One interpretation of these results contends that BAG4 co-expression favors the targeting of active KAT1 channels at the oocyte cell membrane, consistent with what is observed in the experiments described above in yeast.

We next wanted to confirm that the interaction between BAG4 and KAT1 also takes place in plants. To this end, we performed both Bimolecular Fluorescence Complementation (BiFC) and co-immunoprecipitation assays in *Nicotiana benthamiana* infiltrated with *Agrobacterium tumefaciens* containing the appropriate plasmids. As a positive control, we used the KAT1-KAT1 interaction (Fig. 5), observing a uniform fluorescent signal at the plasma membrane. By contrast, we observed a punctate signal corresponding to the KAT1-BAG4 interaction but observed no signal for the corresponding control experiments (Fig. 5). In addition, to add experimental support for this interaction in plants, we performed co-immunoprecipitation experiments upon transient expression in *N. benthamiana*. We were able to efficiently recover BAG4 upon KAT1 immunoprecipitation performed in protein extracts obtained from *N. benthamiana* leaves transiently expressing the two proteins (Fig. 5).

We next performed co-localization experiments to determine the subcellular localization of the KAT1-BAG4 complex. We show that the signal corresponding to the KAT1-BAG4 complex co-localizes with an ER marker protein (ChFP-KDEL), thus lending support to the idea that BAG4 could be involved in KAT1 assembly at this organelle (Fig. 6). Pearson and Mander coefficient analyses indicate a strong degree of co-localization between the KAT1-BAG4 BiFC signal and the ER marker (0.75-0.97 and 0.88-0.99,

194 respectively). By contrast, these same parameters for the KAT1-KAT1 BiFC interaction
195 and the same ER marker indicated no co-localization, as expected (Pearson: -0.17-0.035
196 and Mander: 0.016-0.024). Since the signal for the complex is punctate and is not
197 observed throughout the ER, we also performed co-localization experiments with the
198 ER exit site (ERES) marker Sec24-mRFP and the transmembrane domain of the rat α-2,6-
199 sialyltransferase fused to the Cherry fluorescent protein as a Golgi marker (STtmd-ChFP).
200 We observed co-localization of the KAT1-BAG4 complex with the ERES marker (Pearson:
201 0.43-0.82 and Mander: 0.5-0.98), but not the Golgi marker (Pearson: -0.0039-0.042 and
202 Mander: 0.1-0.5).
203
204 Interestingly, KAT1 was previously shown to interact with Sec24 through its di-acidic ER
205 export signal motif (Sieben et al., 2008). Thus, our data confirm the interaction between
206 BAG4 and KAT1 in a plant model system and show that the KAT1-BAG4 interaction likely
207 takes place at ERES, possibly facilitating its incorporation in coat protein complex II
208 (COPII) vesicles. This is not unexpected as KAT1, like essentially all multi-span plasma
209 membrane proteins, before arriving to the cell surface transits through the ER, where
210 the protein is thought to be assembled into tetramers to form a functional channel that
211 will be inserted into the plasma membrane via the secretory pathway. Our data suggest
212 that BAG4 interacts with KAT1 as it transits through this organelle on its way to the
213 plasma membrane. This model is consistent with that proposed for mammalian BAG
214 proteins that are involved in the regulation of potassium and chloride channels that also
215 act at the ER in cooperation with Hsp70 (Knapp et al., 2014; Hantouche et al., 2017).
216
217 Our results indicate that BAG4 favors KAT1 activity in yeast and oocytes and that the
218 interaction appears to take place at the ER exit sites. We hypothesized that BAG4 acts
219 to facilitate KAT1 transit out of the ER and thus would promote the arrival of active KAT1
220 channels at the plasma membrane. In order to test this model, we examined whether
221 BAG4 influences the arrival of this channel to the plasma membrane. Our first approach
222 was to observe the time course of KAT1 plasma membrane accumulation in the
223 presence and absence of co-expression of BAG4 in *N. benthamiana*. As shown in Figure
224 7, when BAG4 is co-expressed, a higher percentage of KAT1 protein is present at the
225 plasma membrane on day 1 after infiltration, whereas in the absence of BAG4, KAT1

accumulation at the plasma membrane is not comparable to that observed for KAT1_BAG4 until day 3. Figure 7 shows representative images on each day with sufficient signal to clearly visualize KAT1 distribution and the quantification of the percentage of the total KAT1-YFP signal present at the plasma membrane for each condition and time point (n =10 cells). This result is consistent with ectopic BAG4 expression facilitating the assembly of KAT1 containing tetramers and/or their delivery to the plasma membrane, which would in turn favor the accumulation of active channels at the plasma membrane. Since both the yeast and oocyte experiments suggest that BAG4 does not affect overall KAT1 protein accumulation, we tested whether this was also the case in this plant model system. As described in materials and methods, for these transient expression experiments we constructed vectors containing multiple transcriptional units, including an internal control for infiltration efficiency (dsRED containing an HA tag) within the same plasmid. Plants were agroinfiltrated with strains containing KAT1-YFP:dsRED-HA alone or KAT1-YFP:dsRED-HA:BAG4-myc. We analyzed the amount of KAT1-YFP and the internal control (dsRED-HA) in the infiltrated areas using the same time course. As shown in Figure 7, BAG4 co-expression does not increase the steady state amount of KAT1 protein. So, taken together, the data presented in Figures 7 clearly suggest that expression of BAG4 promotes KAT1-YFP arrival at the plasma membrane.

In order to corroborate these observations, we carried out the opposite approach. We investigated the localization of KAT1 in Col-0 wild type plants and in *bag4* mutant lines using transient expression in *A. thaliana* (Fig. 7). Employing the AGROBEST transient transformation protocol (Wu et al., 2014), we observed KAT1 accumulation at the plasma membrane in wild type control plants. However, under the same conditions, in *bag4* mutants, the KAT1 signal observed at the cell surface was markedly decreased and an accumulation of punctate staining was observed (Fig. 7). We could complement this defect of KAT1 plasma membrane targeting observed in the *bag4* mutant by employing vectors co-expressing BAG4 with KAT1. Figure 7 also shows the quantification of the percentage of the total KAT1 signal present at the plasma membrane for each condition tested (n = 10). We observed a much lower percentage of KAT1-YFP at the plasma membrane in *bag4* mutants, as compared to the Col-0 control. Moreover, KAT1-YFP

plasma membrane localization is recovered when we functionally complement the *bag4* mutant. These results support the previous experiments and suggest that the presence of BAG4 promotes the arrival of KAT1 at the plasma membrane, possibly by facilitating its assembly and/or delivery to the cell surface possibly through their physical interaction at the ER exit sites.

In order to provide additional evidence showing that BAG4 is a physiologically relevant KAT1 regulator, we analyzed phenotypes related to KAT1 activity in Arabidopsis lines lacking or overexpressing the *BAG4* gene. Two independent *bag4* mutant lines and two Col-0 lines and one *kat1* line overexpressing *BAG4* were tested for stomatal opening dynamics. The *kat1* and *kat2* single mutants and the *kat1 kat2* double mutant were included for comparison. As shown in Figure 8, two mutant lines lacking the *BAG4* gene show a delay in stomatal opening under all conditions tested. We also observed an initial delay in stomatal opening in the *kat1* and *kat2* mutant lines in response to light treatment, but not potassium-containing opening buffer. Therefore, at high potassium concentrations, the simple mutants are able to open their stomata, likely due to the redundancy of inward rectifying potassium channels. This idea is supported by the phenotype observed for the *kat1 kat2* double mutant, which shows a marked delay in both light and opening buffer. On the other hand, we observed that the overexpression of *BAG4* in Col-0 leads to an increase in stomatal aperture and this response is attenuated in the *kat1* mutant overexpressing *BAG4* (Figure 8). The levels of expression of the BAG4 protein are shown in Supplemental Figure S2.

As a complementary approach, we measured the temperature of the different mutants and BAG4 gain and loss-of-function lines using infrared thermography (Figure 9). Several studies have shown that this technique can be used for analyzing mutants with altered stomatal function as a relationship exists between the temperature of the leaves and variations in stomatal conductance (Jones, 1999; Merlot et al., 2002; Wang et al., 2004). We observed the expected increase in temperature in the lines that showed delayed stomatal aperture dynamics and a decrease in temperature in the Col-0 lines overexpressing BAG4 (Figure 9). When these results are considered together, they strongly suggest that BAG4 plays a physiologically relevant role in regulating potassium

fluxes in stomata and possibly other cells. Importantly, the *BAG4* gene has been reported to be expressed in guard cells, which is a prerequisite for a physiologically relevant KAT1 regulator (Yang et al., 2008).

As discussed above, in the stomatal response assay, we observed additional phenotypes in the *bag4* mutant lines, as compared to the *kat1* or *kat2* simple mutants. These data suggest that BAG4 may regulate proteins in addition to KAT1, including other potassium channels, like KAT2. Lebaudy and collaborators showed the importance of the guard cell membrane inward K^+ channel (GCK_{in}) activity in stomatal movement (Lebaudy et al., 2008), identifying KAT1 and KAT2 as the major contributors. Therefore, we studied whether BAG4 could interact with KAT2 in a BiFC assay in *N. benthamiana*. As shown in Figure 10, we observed a pattern of fluorescence very similar to that observed for the KAT1-BAG4 interaction, but observed no signal in the control combinations. We used the KAT2-KAT1 interaction as a positive control for these assays, showing a uniform interaction at the plasma membrane, similar to what we observed with the KAT1-KAT1 interaction (Figure 5), confirming the functionality of the KAT2 BiFC fusion. Although further studies are required to characterize the molecular details of these interactions and ascertain whether there are additional targets, our data suggest that BAG4 may act as a regulator of at least these two potassium channels and provide a plausible explanation for the results obtained in the stomatal response assays described.

Discussion

The regulation of ion fluxes in guard cells is crucial for stomatal movement, which is an important determinant of the plant's response to fluctuating environmental conditions (Lebaudy et al., 2008). Inward rectifying potassium channels are known to play important roles in this process. As such, these channels are predicted to be highly regulated and as expected, several proteins have been identified as regulators of the KAT1 channel (Sottocornola et al., 2006; Sottocornola et al., 2008; Sato et al., 2009; Eisenach et al., 2012; Ronzier et al., 2014; Zhang et al., 2015; Saponaro et al., 2017). In this report, we describe the identification and initial characterization of a KAT1 regulator that we recovered in a split-ubiquitin screening in yeast. The BAG4 protein was found to

physically interact with KAT1 and also to increase potassium uptake in yeast. In oocytes, a similar phenomenon was observed, as increased KAT1 currents were observed one day after injection. Thus, our data clearly indicate that in two heterologous systems, BAG4 co-expression increases KAT1 transport activity, likely by increasing the number of active channels at the membrane. It is very unlikely that this regulation is at the transcriptional level in these model organisms, since we could show that the total amount of KAT1 does not change upon BAG4 co-expression in yeast and in the oocyte experiments, the same amount of KAT1 cRNA is injected in both cases.

We provide experimental evidence for the physical interaction between KAT1 and BAG4 in plants using two complementary approaches, BiFC and co-immunoprecipitation. The signal corresponding to the KAT1-BAG4 complex co-localizes with a general ER marker and with an ER exit site marker, which supports the notion that BAG4 could be involved in KAT1 assembly at this organelle. BAG4 is a member of a highly conserved family of proteins that all contain a characteristic BAG domain. This domain has been shown to interact with the Hsp70 chaperone in both mammals and plants (Takayama and Reed, 2001; Doukhanina et al., 2006; Kabbage and Dickman, 2008; Lee et al., 2016). On the other hand, Hsp70 has been shown to be required for the assembly of the mammalian potassium channel, hERG1 at the ER (Li et al., 2017). Given the role for the BAG proteins documented in mammals and our observations in yeast and oocytes, we hypothesized that BAG4 may be implicated in the arrival of KAT1 to the plasma membrane, likely at the level of protein folding, tetramer assembly and/or trafficking. We provide experimental evidence supporting this idea using both gain- and loss-of-function experiments, where we observe an improvement in KAT1 plasma membrane arrival upon BAG4 expression and a delay in its accumulation at the plasma membrane in lines lacking the *BAG4* gene. Importantly, we show that the total amount of KAT1 is not affected by BAG4 co-expression, but the percentage of KAT1 that arrives at the plasma membrane is increased. Taken together, these data suggest that the modulation of a step required for KAT1 channel assembly, ER exit and/or plasma membrane delivery may be one of the functions of the BAG4 protein.

Several studies have addressed KAT1 trafficking and its regulation. For example, efficient transport of KAT1 to the plasma membrane is mediated by a di-acidic ER export signal

in the C-terminus of the protein, which binds to the Sec24 component of coat protein complex II (COPII) (Hurst et al., 2004; Meckel et al., 2004; Sieben et al., 2008). Here, we observed the co-localization of the KAT1-BAG4 complex with Sec24, which has been described as a marker of ER exit sites (reviewed in (Matheson et al., 2006; Langhans et al., 2012)). Therefore, BAG4 may regulate this step of KAT1 processing as it moves out of the ER through the secretory pathway towards the plasma membrane. It has also been shown that abscisic acid stimulates the endocytosis of KAT1 in both epidermal and guard cells, which can then recycle back to the plasma membrane when the levels of the hormone decrease (Sutter et al., 2007). In addition, two trafficking related proteins, SYP121 and VAMP721 are involved in regulating KAT1 delivery and recycling, and more recently have been shown to regulate channel gating (Sutter et al., 2006; Eisenach et al., 2012; Zhang et al., 2015; Zhang et al., 2017; Lefoulon et al., 2018). Whether BAG4 is related to any of these known regulatory mechanisms is an interesting question for future studies.

In plants, there are seven members of the BAG family and different phenotypes have been attributed to the *bag1*, *bag4* and *bag6* loss-of-function mutants, suggesting that each family member may carry out distinct functions (Doukhanina et al., 2006; Kabbage et al., 2016; Lee et al., 2016). Moreover, high throughput studies have indicated that, for example, both *BAG4* and *BAG1* are expressed in guard cells, whereas *BAG7* expression is low in this cell type (Winter et al., 2007). In order to study the specificity of the KAT1-BAG4 interaction, we used the split-ubiquitin and functional complementation assays to test whether two other BAG family members that share similar domain architecture, BAG1 and BAG7, interacted with KAT1. Our results show that the BAG protein with a higher level of conservation as compared to BAG4, BAG1 showed a lower, but detectable level of interaction and regulation of KAT1 in yeast. However, a negligible level of interaction was observed for the more distantly related BAG7 protein, thus suggesting a considerable level of specificity for the KAT1-BAG4 interaction.

In order to begin to establish BAG4 as a *bona fide* KAT1 regulator, we tested whether BAG4 may play a role in a physiological response in which this channel is implicated. Indeed, we observed a delay in stomatal aperture in two independent *bag4* mutant lines

in response to external potassium and light. We observed a similar delay in stomatal aperture in response to light in the *kat1* and *kat2* mutant lines. Our data regarding the *kat1* mutant is in contrast to a previous report (Szyroki et al., 2001), but may be explained by differences in the time course studied and/or the mutant lines used. The line used here contains a T-DNA insertion in the first exon. In addition, we observed an increase in stomatal aperture in Col-0 lines overexpressing *BAG4* and this response was reduced when the gene was overexpressed in a *kat1* mutant line. Thus, we were able to show that both loss- and gain-of-function of *BAG4* affects stomatal aperture dynamics and that in the case of *BAG4* overexpression, *KAT1* is required to observe the full response.

We corroborated these results by measuring the temperature of the plants as an indirect measure of the transpiration rate. If the stomatal aperture is decreased in *bag4* mutants, so is the rate of transpiration and therefore, the temperature of the leaves of these plants would be expected to be higher. Our results show that lines lacking the *BAG4* gene display an increased temperature, again adding support to its role in regulating ion fluxes important for stomatal movement. As expected, double mutants lacking both the *KAT1* and *KAT2* genes have a more pronounced phenotype. Moreover, Col-0 lines overexpressing *BAG4* display lower leaf temperatures, which is in agreement with the data regarding stomatal aperture. Taken together, our results establish a role for BAG4 in the regulation of stomatal aperture dynamics through the regulation of the KAT1 inward rectifying potassium channel.

It is interesting to note that the two *bag4* mutant lines showed a longer delay in stomatal opening in response to opening buffer, which was not observed in the *kat1* and *kat2* single mutants but was observed in the *kat1 kat2* double mutant. BAG proteins are very likely to regulate many different proteins and in terms of stomatal aperture, other inward rectifying potassium channels, like KAT2, AKT1, and AKT2/3 are known to contribute to this response and our genetic data suggest a role for KAT2. Thus, we tested whether BAG4 could also interact with KAT2 in plants. Our results using the BiFC assay show a KAT2-BAG4 interaction. Thus, it appears that BAG4 regulates both KAT1 and KAT2, but we cannot rule out other channels as additional targets at this stage.

In mammalian systems, although BAG proteins have been related to many cellular processes, a specific role for BAG proteins in the regulation of ion channels has been reported. Both BAG1 and BAG2 have been shown to regulate the Cystic Fibrosis transmembrane conductance regulator (CFTR) chloride channel and BAG1 was more recently implicated in human Ether-à-go-go-related gene (hERG) potassium channel regulation (Young, 2014; Hantouche et al., 2017). In both cases, it appears that the BAG proteins mediate the misfolded protein response, thus likely playing a role in channel degradation, not plasma membrane delivery. Further experiments will be required to clarify the molecular mechanisms responsible for this apparent difference observed here for the plant BAG4 protein. The Arabidopsis BAG1 protein has been reported to be a co-factor in Hsc70-mediated proteasomal degradation of unimported plastid proteins, and so may have a function more analogous to its mammalian counterparts (Lee et al., 2016). However, our results identify BAG4 as a positive regulator of the KAT1 (and likely KAT2) potassium channel in plants and thus opens a novel line of investigation by linking the plant BAG family to the regulation of potassium channels and stomatal movement.

Conclusions

Taken together, the data presented here suggest that one main role for BAG4 in plants may be related to the post-translational regulation of ion channels and, consequently stomatal movement. Thus, BAG4 may constitute a novel target for the design of engineered crops with altered potassium fluxes, and concomitantly, improved water use efficiency and drought tolerance.

Materials and Methods

Plant materials and plant growth. The following Arabidopsis lines were employed: *kat1* mutant (SALK 093506, carrying the T-DNA insertion in the 1st exon), *kat2* mutant (SALK 025933) and two *bag4* mutant lines SAIL_144_A10 (carrying the T-DNA insertion in the 1st exon) and SALK_033845 (carrying the T-DNA insertion in the 2nd exon) (obtained from the Salk Institute Genomic Analysis Laboratory and (Sessions et al., 2002). Arabidopsis plants were grown under an 8h light: 16h dark photoperiod at 22 ºC in MS media supplemented with 1% sucrose. For stomatal movement and leaf temperature assays, after 2 weeks, plants were transplanted to soil and analyzed at 4-6 weeks. *Nicotiana benthamiana* plants were grown for 4-5 weeks in soil under an 16h light: 8h dark photoperiod at 24 ºC.

Yeast strains and plasmids. The Split-ubiquitin KAT1 bait vector used for the screening was derived from the KAT1-pMetYCgate vector (ABRC CD3-815, (Obrdlik et al., 2004)). In order to carry out the screening, the AMP^r marker was substituted with KAN^r by recombination in yeast as follows: the kanamycin resistance gene was amplified with the primers Kan-F 5'-ttcttgaagacgaaagggcctcgtgatacgcctattTCCAGTTCGATTTATTC AACAAAG-3' and Kan-R 5'-taaagtatatatgagtaaacttggtctgacagttacGATCGATCCTAG TAAGCCACGTTG-3' and was co-transformed in the PLY240 strain (MATa *his3*Δ200 *leu2*-3,112 *trp1*Δ901 *ura3*-52 *suc2*Δ9 *trk1*Δ51 *trk2*Δ50::lox-KanMX-lox; (Bertl et al., 2003) together with the KAT1-pMETYCgate vector linearized with AatII. Clones growing in media lacking leucine were tested for growth in media containing 50 mM LiCl to select strains expressing KAT1. Plasmids were recovered from these yeast strains and transformed into DH5α and kanamycin resistant colonies were selected. The resulting plasmid was confirmed by sequencing. The cDNA library from 6-day-old *Arabidopsis thaliana* seedlings in the pDSL-Nx vector was obtained from Dualsystems Biotech AG. The screening was carried out in the THY.AP4 strain (MATa, *ura3*, *leu2*, lexA::lacZ::*trp1*, lexA::*HIS3*, lexA::*ADE2*; (Paumi et al., 2007)). The BAG4 clone recovered in the screening lacks the sequence encoding the first 13 amino acids. The BAG1, BAG7 and full-length BAG4 plasmids were constructed by recombination into the pDSL-Nx vector in yeast using PCR products amplified from a cDNA library made from Arabidopsis seedlings.

Split-ubiquitin screening. The THY.AP4 strain containing the modified KAT1-Cub (KAT1-CubKAN^r) plasmid was transformed with 20 micrograms of the *A. thaliana* cDNA library in the pDLSN-X vector (Dual Systems). Approximately 8.6 x 10^6 transformants were analyzed for growth in selective media. The first 125 colonies growing in selective media were analyzed. Plasmids were recovered, re-transformed, tested for growth in selective media, classified by restriction analysis and subjected to specificity tests using the Ost3-Cub vector encoding a yeast oligosaccharyl transferase (Yan et al., 2005). The clones that passed these tests were then sequenced and analysed in the yeast functional complementation assay.

Functional complementation assay in yeast. The PLY240 strain was co-transformed with the KAT1-CubKAN^r and the indicated pDLSN-X vectors and the empty vector corresponding controls. Pre-cultures were grown to saturation in SD media supplemented with auxotrophic requirements, 0.75 mg/mL methionine (to reduce KAT1 expression) and 0.1 M KCl. Fresh cultures (1:20 dilution) were grown for 16 hours in low potassium Translucent media supplemented with requirements and methionine (ForMedium™ UK; (Navarrete et al., 2010)) and diluted to OD_{600} 0.2 in three different conditions of Translucent media supplemented with auxotrophic requirements: 1) low potassium, no methionine (low KCl, high KAT1 expression); low potassium, 0.75 mg/mL methionine (low KCl, low KAT1 expression) and 3) 0.1 M KCl, no methionine (high KCl, high *KAT1* expression). The Translucent media contains 12 µM K^+. The optical density was determined periodically for 72 hours using a BioscreenC system (Oy Growth Curves Ab Ltd). Triplicate determinations were performed for at least 3 independent transformants for each plasmid combination. Similar results were observed in all experiments. Correct expression of each fusion protein was confirmed by immunoblot analysis of the corresponding whole cell extracts of cultures grown in Translucent media supplemented with 0.1 M KCl and 0.75 mg/mL methionine using anti-HA and anti-LexA antibodies (Covance and Abcam, respectively), the corresponding anti-mouse or anti-rabbit HRP secondary antibodies and ECL detection system (GE Healthcare). Several independent clones were used for the quantification of KAT1 protein expression in the absence and presence of BAG4. ImageJ was used to quantify the bands corresponding to the LexA signal and the loading control to calculate normalized KAT1 expression.

Potassium consumption uptake and external acidification in yeast. The indicated plasmids were transformed in the PLY240 background and grown as described above in the functional complementation assay to mid-log phase OD600 = 0.5-0.6 in Translucent media supplemented with auxotrophic requirements and 0.75 mg/mL methionine. Cells were collected by centrifugation, washed, resuspended in sterile water and incubated for 30 minutes at room temperature. External K^+ was monitored using external K^+-selective mini-electrodes. Single-barrelled borosilicate glass capillaries, 7 cm long and of 1.5 mm of external diameter, were pulled in a patch clamp puller to get an open tip. Then, capillaries were sylanized and back-filled with K^+ ionophore I sensor (cocktail B, cat. No. 60398; Fluka, now part of Sigma) dissolved in a mixture of polyvinyl-chloride/tetrahydrofuran (40 mg/mL) at a ratio of 30:70 (v/v), as was previously described (Planes et al., 2015). For the assays, approximately 20 mg of cells (wet weight) were resuspended in 3 mL of 10 mM MES pH 4.0 and loaded in a temperature controlled (20 °C) plexiglass cylinder chamber under continuous stirring. K^+-selective and reference electrode tips were placed in the assay medium and connected to a high-impedance differential amplifier (FD223; World Precision Instruments). In addition, a single glass pH electrode (model 5209, Crison) was also submerged into the assay medium in order to measure the external acidification to check the activation of the proton ATPase. After steady readings of both pH and external potassium K^+ signals were obtained, potassium chloride was added to a final concentration of 1 mM and then, after stable readings values were again attained, 20 mM of glucose were added to activate the proton ATPase, Pma1 and energize potassium uptake. Both the external pH and the potassium concentration were recorded for 45 minutes after glucose addition. The K^+ electrode signal was calibrated before and after experiments by adding potassium chloride to final concentrations of 0.1, 0.5, 1 and 10 mM in the assay media. Calibration curves render slopes around 45 mV per pK^+ unit. Both the total uptake (after 45 minutes) and the initial rate of K^+ uptake (slope of the curve representing the initial uptake; 5-8 minutes) were determined for three independent clones of each plasmid combination indicated (Figures 3A and B, respectively).

Two-electrode voltage clamp in Xenopus oocytes. KAT1 and BAG4 coding regions were cloned into a modified pGEM-HE vector (D. Becker, University of Würzburg, Germany).

cRNA were synthesized from 1 µg of linearized vector using the HiScribe™ T7 ARCA mRNA (with tailing) kit (NEB, http://www.NEB.com). Oocytes were obtained and prepared as previously described (Véry et al., 1995) and were injected with 30 ng of KAT1 cRNA or co-injected with 30 ng of KAT1 cRNA and 22.5 ng of BAG4 cRNA using a pneumatic injector. One day after oocyte injection, currents from whole oocytes bathed in K100 medium (100 mM KCl, 2 mM $MgCl_2$, 1 mM $CaCl_2$, 10 mM HEPES/Tris pH 6) were recorded using the two-electrode voltage clamp technique. Data acquisition and analyses were performed as previously described (Corratgé-Faillie et al., 2017). Voltage drops resulting from the series resistance of the bath were corrected by using two external electrodes connected to a bath probe (VG-2A x100 Virtual-ground bath clamp; Axon Instruments). KAT1 currents were obtained by subtraction of mean currents recorded in water-injected oocytes from the same oocyte batch. The percentage of KAT1 current increase with BAG4 = Mean current in the presence of BAG4 - Mean current in its absence / Mean current in its absence.

BiFC and co-immunoprecipitation assays in Nicotiana benthamiana. All *KAT1* and *BAG4* plasmids used for the BiFC and co-immunoprecipitation experiments and to generate overexpression lines were constructed using the GoldenBraid system (Sarrion-Perdigones et al., 2013). For BiFC assays, we used pUPD2 vectors containing the YFN or YFC sequences from the GoldenBraid collection. Then, we cloned *KAT1* and *BAG4* versions, compatible with the cloning system into the pUPD2 vector. Alpha vectors containing the indicated fusion proteins and the 35S promoter and Tnos terminator were assembled and combined to generate the omega level plasmids that were transformed into the *Agrobacterium tumifaciens* strain C58Ci. For indicated experiments, alpha level plasmids were constructed from these omega plasmids to generate constructs containing 3 or 4 transcriptional units. For plant infiltration, we used 4- to 5-week-old *N. benthamiana* plants grown at 24 ºC under a 16h light: 8h dark photoperiod. For co-localization experiments used to determine the subcellular localization of the complex, the *KAT1-BAG4* interacting combination was co-infiltrated with a second plasmid containing either the ER marker (calreticulin targeting sequence-Cherry fluorescent protein-KDEL retention sequence (ChFP-KDEL)), the Sec24-RFP ER exit site (ERES) marker (both kindly provided by V. Pallás, IBMCP, Spain), or the

transmembrane domain of the rat α-2,6-sialyltransferase enzyme fused to the Cherry fluorescent protein as a Golgi marker (STtmd-ChFP) (Prokhnevsky et al., 2005). An agrobacterium strain (C58Ci) transformed with the plasmid encoding the P19 Tomato Bushy Stunt Virus silencing suppressor was also used in all the infiltrations (Sarrion-Perdigones et al., 2013). The images were acquired using a Zeiss fluorescence confocal microscope with the following settings: YFP was excited with an Argon laser (514 nm) and detected at 516-548 nm. Cherry, RFP and dsRED fluorescent proteins were excited using the DPSS 561-10 laser (561 nm) and detected at 580-650 nm. Chloroplast autofluorescence was detected between 675 and 760 nm. The statistical analyses for KAT1-BAG4 BiFC and the organelle makers were determined by calculating the Pearson and Mander coefficients (corresponding to the range of values obtained in 4 independent images) (Dunn et al., 2011). For co-IP assays, we used a pUPD2 4x-*c-myc* sequence from the Addgene collection, to create the c-myc-BAG4 fusion. We combined the *KAT1*-YFP and c-myc-*BAG4* alpha vectors to build the omega plasmid containing both fusion proteins and infiltrated *N. benthamiana* leaves. Extraction of total proteins was carried out in modified PBS buffer (140 mM NaCl, 8 mM $Na_2HPO_4 \cdot 7H_2O$, 2 mM KH_2PO_4, 10 mM KCl, Proteinase Inhibitor, pH 7.4). The KAT1-YFP protein was purified using the GFP-trap (GFP-Trap®_MA, Chromotech) according to the manufacturer's instructions. Samples of the protein extracts, the unbound material and the KAT1 purification were separated on 8% SDS-PAGE gels, transferred to nitrocellulose membranes and probed with an anti-GFP antibody (clone 7.1 and 13.1 mixture, Roche) and an anti-*c-myc* antibody (clone 9E10, Roche) to detect BAG4. Immune complexes were visualized using the corresponding anti-mouse or anti-rabbit HRP secondary antibodies and ECL detection system (GE Healthcare).

Kinetics of plasma membrane accumulation in N. benthamiana and A. thaliana

For transient expression in *N. benthamiana*, leaves were infiltrated, treated and imaged as described for BiFC and Co-IP. However, in this case P19 silencing suppressor was not added to the infection mixture. The ImageJ program was used to quantify the percentage of KAT1-YFP present at the plasma membrane as follows: the free draw tool was used to trace the contour of individual cells, directly adjacent to the cell boarder (inside cell fluorescence). These forms were digitally enlarged by 7 pixel units using the

ImageJ tool to quantify the whole cell fluorescence. Fluorescence levels in ellipses adjacent to the cells were also quantified and used as the background measurement. The corrected total cell fluorescence (CTCF) was calculated using the following formula: Integrated Density – (area of selected cell × mean fluorescence of background readings). The percentage of fluorescence signal at the plasma membrane was then calculated using the following formula: $\%\,\text{fluorescence PM} = 100 - \left(\frac{\text{CTF inside fluorescence}}{\text{CTF whole cell fluorescence}} * 100\right)$. This procedure was carried out for 10 individual cells from each of the indicated conditions deriving from experiments done on different days. In order to quantify the amount of KAT1 protein with and without BAG4 co-expression, an alpha1 level plasmid was constructed to combine the KAT1-YFP_myc-BAG4 omega construct (or the control) with the dsRED protein which incorporates an HA epitope tag (dsRED-HA) in the same vector. In this way, the amount of dsRED can be used as an internal control monitoring the level of transient expression in each case because all transcriptional units are in the same plasmid. Infected plants were observed on days 1, 2 and 3 post-infiltration by fluorescence confocal microscopy and whole cell protein extracts were generated from the infiltrated material by grinding 2 cm leaf discs in SDS-PAGE loading buffer. Samples were separated on SDS-PAGE, transferred and KAT1, BAG4 and dsRED were detected using anti-GFP, anti-c-myc and anti-HA antibodies.

For transient expression in Arabidopsis, the Col-0 control and the *bag4* mutant lines (SALK_033845 and SAIL_144_A10) were agroinfiltrated following the AGROBEST protocol (Wu et al., 2014). The plasmid used was the alpha level plasmid containing KAT1-VENUS$_{intron}$ which included an intron in the Venus sequence (kindly provided by Stan Gelvin, Purdue University, USA). This was required to avoid expression of the KAT1 fusion protein in the agrobacterium strain. An omega vector combining the KAT1-VENUS$_{intron}$ and myc-BAG4 transcriptional units was used for the complementation assays. Confocal images were acquired as described above using the 514 laser and an emission wavelength between 515 nm and 530 nm. The quantification of the amount of KAT1-YFP at the plasma membrane was calculated as described above for 10 individual cells from each condition indicated.

Stomatal movement assays. The following lines were employed: *kat1* mutant (SALK 093506, carrying the T-DNA insertion in the 1st exon), *kat2* mutant (SALK 025933) and the two *bag4* mutant lines SAIL_144_A10 (carrying the T-DNA insertion in the 1st exon) and SALK_033845 (carrying the T-DNA insertion in the 2nd exon) (obtained from the Salk Institute Genomic Analysis Laboratory and (Sessions et al., 2002), two independent transformants that are homozygous for the *BAG4* insertion in the Col-0 and *kat1* mutant (SALK 093506, carrying the T-DNA insertion in the 1st exon) lines generated by the floral dipping method using an omega level plasmid containing the c-myc-BAG4 fusion and the BASTA resistance gene. The double *kat1 kat2* mutant was generated by crossing the single mutants listed above. Plants were grown 4-6 weeks under an 8h light: 16h dark photoperiod at 22 ºC. Five leaves (each taken from different plants) from each genotype and condition were analysed. For the dark conditions, leaves were harvested 1 hour before the lights switched on and the leaf was split into two halves: one was maintained in the dark in MES solution, while the other was incubated in stomatal opening buffer (10 mM KCl, 7.5 mM iminodiacetic acid; 10 mM MES/Tris pH 6.2), for 2.5 hours. For light treatment, the leaf was split into two halves and both were kept in 10 mM MES (pH 5.6). One half was kept in the dark and the other exposed to light and observed 2.5 hours later. To take stomatal images, the tissue was mounted on a microscope slide and immersed in the respective solution. The stomatal aperture was defined as the ratio between the length of the stomatal aperture from the point of junction of the inner lips and the maximal width between the inner cuticular lips. For each condition, between 60 and 100 stomata were analyzed in five different plants. The entire assay was repeated three times.

Leaf temperature measurements. The same lines used in the stomatal movement assays were grown under an 8h light: 16h dark photoperiod at 22 ºC. The thermographic camera Bosch GTC 400 C was used to generate the infrared images of the plants 1.5 hours after the lights turned on. The plants were sown in individual pots such that the rosette leaves were not touching the walls of the pot, the tray or other plants. For imaging, each plant was moved to a tray partially filled with water, to create a uniform environmental temperature around the pot. Leaf temperature was calculated using the

GTC Transfer Software. A total of 6 plants were measured for each genotype. Ten points were measured for each plant (60 data points/genotype). Data from each genotype were pooled together and statistically analyzed (Student *t*-test) using the Graph Prism6 software.

Accession Numbers

Sequence data from this article can be found in the GenBank data libraries under accession numbers: *AtKAT1,* At5g46240; *AtKAT2,* At4g18290; *AtBAG4,* At3g51780. Mutants used in this article can be obtained from the Arabidopsis Biological Resource Center under the following accession numbers: *kat1* mutant (SALK 093506), *kat2* mutant (SALK 025933), and *bag4* mutant lines (SAIL_144_A10) and (SALK_033845).

Supplemental Data

Supplemental Figure S1. BAG4 co-expression favors early activity of KAT1 in Xenopus oocytes.

Supplemental Figure S2. Immunodetection of myc-BAG4 protein in homozygous transgenic lines.

Acknowledgements

The authors would like to thank Elena Moreno, María José Falaguer, Alejandro Mossi, Sara Aljama, José Antonio Navarro, Vicente Pallás, Daniel Franco-Aragón, Jorge Lozano, and Stan Gelvin for assistance in the completion of this work and for providing reagents.

682 **Figure Legends**

683 **Figure 1. Effect of the co-expression of interacting proteins on the functional**
684 **complementation by KAT1 in yeast.** A) The indicated plasmids were co-transformed in
685 the *trk1 trk2* mutant strain (PLY240) and the growth of the strains was assayed as
686 described in Materials and Methods using the Translucent media (which contains 12 µM
687 potassium) with or without methionine supplementation to decrease the expression of
688 KAT1 (under control of the *MET25* promoter). The graph shows the average value of the
689 optical density at 72 hours for triplicate determinations and the experiment was done
690 with at least 3 independent transformants for each plasmid combination. (Translucent
691 media with no KCl supplementation = Low KCl (12 µM K^+); Translucent media containing
692 0.75 mg/mL methionine = Low KAT1; Translucent media + 50 mM KCl added = High KCl;
693 Translucent media -/+ KCl without methionine = High KAT1). Data presented are the
694 mean ±SD and similar results were observed for three independent transformants.
695 Asterisks (**) indicate statistical significance (Student *t*-test) with a p value < 0.01. B)
696 Immunoblot analysis of protein extracts from the indicated strains showing the correct
697 expression of each of the fusion proteins. The KAT1 bait vector protein is detected with
698 the anti-LexA antibody and the prey proteins with the anti-HA antibody. Results for a
699 representative clone are shown. The long exposure is included to visualize the
700 expression of the RPT2 prey protein, which accumulates less than the other two prey
701 proteins. C) The KAT1 signal and the corresponding loading control were quantified
702 using the ImageJ software and the average values of KAT1/loading control (Normalized
703 KAT1) was calculated for 6 control strains (KAT1_empty vector) and 7 KAT1_BAG4
704 strains. Data presented are the mean ±SD.
705
706 **Figure 2. Study of the specificity of the interaction between KAT1 and other BAG family**
707 **members.** A) The indicated plasmids were transformed into the THY.AP4 strain and
708 grown to saturation in selective media. Serial dilutions were spotted onto media with
709 the indicated composition to test for the protein-protein interaction between KAT1 and
710 the indicated BAG family proteins. Identical results were observed for four independent
711 clones. B) Immunoblot analysis of protein extracts from the indicated strains showing
712 the correct expression of each of the fusion proteins. The KAT1 bait protein is detected

with the anti-LexA antibody and the prey proteins with the anti-HA antibody. Results for a representative clone are shown. C) The indicated plasmids were co-transformed in the *trk1 trk2* mutant strain (PLY240) and the growth of the strains was assayed as described in Figure 1A. The average value of triplicate determinations of the optical density of the growth normalized to the potassium-supplemented media is shown for each strain. Data presented are the mean ±SD and similar results were observed for 3 independent clones of each plasmid combination. Asterisks (***) indicate statistical significance (Student *t*-test) with a p value < 0.001 compared to the KAT1_ø control strain.

Figure 3. Potassium uptake and external acidification. The indicated plasmids were co-transformed in the *trk1 trk2* mutant strain (PLY240) and the strains were grown in low KCl and low KAT1 conditions and processed as described in Materials and Methods. A) The bars represent the average value for three independent experiments for the total potassium uptake for 45 minutes expressed as µmol K^+/mg cells ±SD. B) The bars represent the average value for three independent experiments for the initial rate of potassium uptake expressed as µmol K^+/min*mg cells calculated using the slope of the depletion curve (first 5-18 minutes) normalized to the wet weight of the cells ±SD. C) The bars represent the average value for three independent experiments of the change in the pH value measured in parallel with the potassium consumption ±SD. The change in the external pH was determined during the first 15 minutes after glucose addition and was normalized to the wet weight of the cells. Asterisks (*) indicate statistical significance (Student *t*-test) with a p value < 0.05.

Figure 4. BAG4 co-expression increases KAT1 current in *Xenopus* oocytes. A) Voltage-clamp protocol and representative current traces recorded by two-electrode voltage clamp in the presence of 100 mM KCl on oocytes co-expressing KAT1 or KAT1 and BAG4. B) KAT1 current (I) –voltage (V) relationships of oocytes co-expressing KAT1 and BAG4 (white circles) or expressing KAT1 alone (black circles). Data are means ± SE (n=7 for KAT1, n=11 for KAT1 + BAG4), and are representative of three experiments performed on different oocyte batches. C) Increase of mean KAT1 current upon BAG4 co-expression, at -110 mV (black) and at -155 mV (grey). Mean currents are from B). D) Voltage-dependence of KAT1-current activation in the presence of BAG4 (white circles)

or with KAT1 expressed alone (black circles). Gating parameters (z, gating charge, and Ea50, half-activation potential) were estimated by performing fits to the KAT1 I-V relationships (in the presence or absence of BAG4) with a Boltzmann function coupled to a linear relation (Lebaudy et al., 2010). G, KAT1 macroscopic conductance (G = I/V); G_{max}, KAT1 macroscopic conductance at infinitely negative voltage.

Figure 5. Confirmation of the interaction between KAT1 and BAG4 in *N. benthamiana*. Agrobacterium strains harbouring the indicated plasmids were used to infiltrate *N. benthamiana* leaves and images were obtained using fluorescence confocal microscopy 72 hours post-infiltration. A) Representative BiFC images for the KAT1-KAT1 interaction and control plasmids. The overlay of the grey scale and BiFC fluorescence is shown. Leaf epithelial cells and stomata are visible. B) Representative BiFC images for the KAT1-BAG4 interaction. Representative images of the experiments performed with the control plasmids are shown below. The red signal corresponds to chloroplast autofluorescence. For panels A and B, similar results were observed in at least four independent experiments performed on different days. (Bar = 20μm) C) Agrobacterium strains expressing the indicated plasmids were used to infiltrate *N. benthamiana* leaves. Samples were taken at 72 hours post-infiltration and processed for protein extraction and co-immunoprecipitation as described in Materials and Methods. The figure shows the results of the immunodetection using antibodies that recognize the BAG4 and KAT1 proteins. The amount of BAG4 recovered in the KAT1 purification is shown in the first lane on the left. Similar results were observed in two independent experiments performed on different days. (YFN = N-terminal part of YFP; YFC=C-terminal part of YFP; IP=immunoprecipitation; FT=flow through).

Figure 6. The KAT1-BAG4 complex co-localizes with the ER and ERES markers. A) A plasmid containing the KAT1-BAG4 BiFC interaction and the ER marker ChFP-KDEL were infiltrated as described. The BiFC signal (right), ChFP signal (center), and the overlay image of the grey scale, BiFC fluorescence and the ChFP signals (left) are shown. Leaf epithelial cells and stomata are visible. B and C) The same co-localization analysis of the KAT1-BAG4 complex was performed with the ER exit site marker, Sec24 fused to RFP (Sec24-RFP) (B) and the STtmd-ChFP Golgi marker (C). The yellow arrows indicate the

775 points of co-localization with the ER marker. Chloroplast autofluorescence is shown in
776 blue. (Bar = 20μm). (YFN = N-terminal part of YFP; YFC=C-terminal part of YFP;
777 ChFP=Cherry Fluorescent Protein; RFP=Red Fluorescent Protein; STtmd-ChFP= rat α-2,6-
778 sialyltransferase transmembrane domain fused to the Cherry fluorescent protein).
779
780 **Figure 7. BAG4 expression effects the subcellular localization of KAT1.** A) Plasmids
781 containing KAT1-YFP or both KAT1-YFP and BAG4 were transiently expressed in *N.*
782 *benthamiana* using agro-infiltration. The fluorescence signal was analysed by confocal
783 microscopy 1-, 2- and 3-days post-infiltration. Representative images are shown. Leaf
784 epithelial cells and stomata are visible. Similar results were observed in three
785 independent experiments performed on different days. (Bar = 20μm) B) The percentage
786 of the fluorescence signal present in the plasma membrane (PM) was quantified using
787 ImageJ, as described in Materials and Methods. The graph shows the average values ±SD
788 for 10 cells for each condition tested. C) Similar experiments as described in panel A
789 were performed, but using GoldenBraid plasmids containing KAT1-YFP:dsRED-HA or
790 KAT1-YFP:myc-BAG4:dsRED-HA. Whole cell extracts were prepared from infiltrated
791 areas (previously confirmed to express KAT1-YFP) and proteins were processed for
792 immunodetection. The dsRED-HA protein serves as an internal control for the efficiency
793 of transient expression. (DAY PI= Day post-infiltration). D) The KAT1-VENUS$_{intron}$ (KAT1-
794 VENUS$_i$, top row) or the KAT1-VENUS$_{intron}$_BAG4 (bottom row) plasmids were transiently
795 expressed in the Col-0 and the *bag4* mutant Arabidopsis lines using agro-infiltration. The
796 fluorescence signal was analyzed by confocal microscopy 2 days after infiltration.
797 Representative images are shown and similar results were observed in three
798 independent experiments. Leaf epithelial cells and stomata are visible. (Bar = 20μm). E)
799 The percentage of the fluorescence signal present in the plasma membrane (PM) was
800 quantified using ImageJ, as described in Materials and Methods. The graph shows the
801 average values ±SD for 10 cells for each condition tested. (Student *t*-test) (**: p value
802 <0.01).
803
804 **Figure 8. Effect of BAG4 loss and gain-of-function on stomatal aperture.** Stomata from
805 the indicated Arabidopsis lines were analyzed as described in Materials and Methods.
806 The data show the average ratio for 60-100 stomata ±SD. A) The width/length ratio of

807 stomata of the different mutant lines were determined in leaves from the indicated lines
808 harvested 1 hour before the lights turned on (Dark), incubated for 2.5 hours in opening
809 buffer in the dark (Opening buffer, O.B.) or 2.5 hours after the lights turned on (Light).
810 Similar results were observed in three independent experiments. B) The width/length
811 ratio of stomata of control lines and Col-0 and *kat1* homozygous for 35S:*BAG4* transgene
812 were determined as described in panel A. For both experiments, the asterisks indicate
813 statistical significance as compared to the Col-0 dark control (Student *t*-test) (**: p value
814 <0.01; ***: p value < 0.001; **** p value < 0.0001). The length/width ratio was also
815 significantly increased in *BAG4* overexpressing lines in both light and opening buffer (#
816 indicates statistical comparison with Col-0 O.B. and ▪ indicates statistical comparison
817 with Col-0 light).
818
819 **Figure 9. Effect of BAG4 loss and gain-of-function on leaf temperature.** The same lines
820 described in Figure 8 were analyzed for leaf temperature using an infrared
821 thermography, as described in Materials and Methods (Panel A mutant lines, Panel B
822 35S:*BAG4* lines). Each symbol represents an individual measurement and the bar
823 represents the average value for 10 measurements of 6 different plants for each
824 genotype. The error bars represent the standard deviation. For both experiments, the
825 asterisks indicate statistical significance as compared to the Col-0 control or the
826 comparisons indicated by the brackets above the graphs (Student *t*-test) (**: p value
827 <0.01; ***: p value < 0.001; **** p value < 0.0001).
828
829 **Figure 10. BAG4 interacts with KAT2 in BiFC assays in *N. benthamiana*.** Interaction
830 assays were carried out and analyzed as described in the legend to Figure 5. Leaf
831 epithelial cells and stomata are visible. As shown, a similar pattern of interaction is
832 observed for KAT2 when tested with BAG4 (compare with Figure 5B). The BiFC signals
833 corresponding to the KAT2-KAT1 and KAT2-BAG4 interactions are shown in green and
834 the chloroplast autofluorescence is shown in red. (YFN = N-terminal part of YFP; YFC=C-
835 terminal part of YFP). (Bar = 20μm).
836
837

Literature Cited

Anderson JA, Huprikar SS, Kochian L V, Lucas WJ, Gaber RF (1992) Functional expression of a probable Arabidopsis thaliana potassium channel in Saccharomyces cerevisiae. Proc Natl Acad Sci U S A **89**: 3736–3740

Bertl A, Ramos J, Ludwig J, Lichtenberg-Fraté H, Reid J, Bihler H, Calero F, Martínez P, Ljungdahl PO (2003) Characterization of potassium transport in wild-type and isogenic yeast strains carrying all combinations of trk1, trk2 and tok1 null mutations. **47**: 767–780

Doukhanina E V., Chen S, Van Der Zalm E, Godzik A, Reed J, Dickman MB (2006) Identification and functional characterization of the BAG protein family in Arabidopsis thaliana. J Biol Chem. doi: 10.1074/jbc.M511794200

Dreyer I, Antunes S, Hoshi T, Müller-Röber B, Palme K, Pongs O, Reintanz B, Hedrich R (1997) Plant K+ channel alpha-subunits assemble indiscriminately. Biophys J **72**: 2143–2150

Duby G, Hosy E, Fizames C, Alcon C, Costa A, Sentenac H, Thibaud JB (2008) AtKC1, a conditionally targeted Shaker-type subunit, regulates the activity of plant K+ channels. Plant J **53**: 115–123

Dunn KW, Kamocka MM, McDonald JH (2011) A practical guide to evaluating colocalization in biological microscopy. Am J Physiol Cell Physiol **300**: C723-42

Eisenach C, Chen ZH, Grefen C, Blatt MR (2012) The trafficking protein SYP121 of Arabidopsis connects programmed stomatal closure and K^+ channel activity with vegetative growth. Plant J **69**: 241–251

Gierth M, Mäser P (2007) Potassium transporters in plants – Involvement in K+ acquisition, redistribution and homeostasis. **581**: 2348–2356

Grefen C, Chen Z, Honsbein A, Donald N, Hills A, Blatt MR (2010) A novel motif essential for SNARE interaction with the K(+) channel KC1 and channel gating in Arabidopsis. Plant Cell **22**: 3076–3092

Hantouche C, Williamson B, Valinsky WC, Solomon J, Shrier A, Young JC (2017) Bag1 Co-chaperone Promotes TRC8 E3 Ligase-dependent Degradation of Misfolded Human Ether a Go-Go-related Gene (hERG) Potassium Channels. J Biol Chem **292**: 2287–2300

Hoang TM, Moghaddam L, Williams B, Khanna H, Dale J, Mundree SG (2015) Development of salinity tolerance in rice by constitutive-overexpression of genes involved in the regulation of programmed cell death. Front Plant Sci **6**: 175

Honsbein A, Blatt MR, Grefen C (2011) A molecular framework for coupling cellular volume and osmotic solute transport control. J Exp Bot **62**: 2363–2370

Hurst AC, Meckel T, Tayefeh S, Thiel G, Homann U (2004) Trafficking of the plant potassium inward rectifier KAT1 in guard cell protoplasts of Vicia faba. Plant J **37**: 391–397

Ivashikina N, Becker D, Ache P, Meyerhoff O, Felle HH, Hedrich R (2001) K(+) channel profile and electrical properties of Arabidopsis root hairs. FEBS Lett **508**: 463–469

Jeanguenin L, Alcon C, Duby G, Boeglin M, Chérel I, Gaillard I, Zimmermann S, Sentenac H, Véry AA (2011) AtKC1 is a general modulator of Arabidopsis inward Shaker channel activity. Plant J **67**: 570–582

878 **Jiang Y, Lee A, Chen J, Ruta V, Cadene M, Chait BT, MacKinnon R** (2003) X-ray structure of a
879 voltage-dependent K+ channel. Nature **423**: 33–41

880 **Jones HG** (1999) Use of thermography for quantitative studies of spatial and temporal
881 variation of stomatal conductance over leaf surfaces. Plant, Cell Environ **22**: 1043 –1055

882 **Kabbage M, Dickman MB** (2008) The BAG proteins: A ubiquitous family of chaperone
883 regulators. Cell Mol Life Sci **65**: 1390–1402

884 **Kabbage M, Kessens R, Dickman MB** (2016) A plant Bcl-2-associated athanogene is
885 proteolytically activated to confer fungal resistance. Microb Cell **3**: 224–226

886 **Knapp RT, Wong MJH, Kollmannsberger LK, Gassen NC, Kretzschmar A, Zschocke J, Hafner K,**
887 **Young JC, Rein T** (2014) Hsp70 cochaperones HspBP1 and BAG-1M differentially regulate
888 steroid hormone receptor function. PLoS One **9**: doi:10.1371/journal.pone.0085415

889 **Langhans M, Meckel T, Kress A, Lerich A, Robinson DG** (2012) ERES (ER exit sites) and the
890 "Secretory Unit Concept." J Microsc **247**: 48–59

891 **Lawson T, Blatt MR** (2014) Stomatal size, speed, and responsiveness impact on photosynthesis
892 and water use efficiency. Plant Physiol **164**: 1556–1570

893 **Lebaudy A, Pascaud F, Véry AA, Alcon C, Dreyer I, Thibaud JB, Lacombe B** (2010) Preferential
894 KAT1-KAT2 heteromerization determines inward K+ current properties in Arabidopsis
895 guard cells. J Biol Chem **285**: 6265–6274

896 **Lebaudy A, Vavasseur A, Hosy E, Dreyer I, Leonhardt N, Thibaud JB, Véry AA, Simonneau T,**
897 **Sentenac H** (2008) Plant adaptation to fluctuating environment and biomass production
898 are strongly dependent on guard cell potassium channels. Proc Natl Acad Sci U S A **105**:
899 5271–5276

900 **Lee DW, Kim SJ, Oh YJ, Choi B, Lee J, Hwang I** (2016) Arabidopsis BAG1 Functions as a Cofactor
901 in Hsc70-Mediated Proteasomal Degradation of Unimported Plastid Proteins. Mol Plant **9**:
902 1428–1431

903 **Lefoulon C, Waghmare S, Karnik R, Blatt MR** (2018) Gating control and K. Plant Cell Env **41**:
904 2668–2677

905 **Li K, Jiang Q, Bai X, Yang YF, Ruan MY, Cai SQ** (2017) Tetrameric Assembly of K+ Channels
906 Requires ER-Located Chaperone Proteins. Mol Cell **65**: 52–65

907 **Long SB, Campbell EB, Mackinnon R** (2005) Crystal structure of a mammalian voltage-
908 dependent Shaker family K+ channel. Science (80-) **309**: 897–903

909 **Mäser P, Thomine S, Schroeder JI, Ward JM, Hirschi K, Sze H, Talke IN, Amtmann A, Maathuis**
910 **FJ, Sanders D, et al** (2001) Phylogenetic relationships within cation transporter families of
911 Arabidopsis. Plant Physiol **126**: 1646–1667

912 **Matheson LA, Hanton SL, Brandizzi F** (2006) Traffic between the plant endoplasmic reticulum
913 and Golgi apparatus: to the Golgi and beyond. Curr Opin Plant Biol **9**: 601–609

914 **Meckel T, Hurst AC, Thiel G, Homann U** (2004) Endocytosis against high turgor: intact guard
915 cells of Vicia faba constitutively endocytose fluorescently labelled plasma membrane and
916 GFP-tagged K-channel KAT1. Plant J **39**: 182–193

917 **Merlot S, Mustilli AC, Genty B, North H, Lefebvre V, Sotta B, Vavasseur A, Giraudat J** (2002)

Use of infrared thermal imaging to isolate Arabidopsis mutants defective in stomatal regulation. Plant J **30**: 601–609

Mumberg D, Müller R, Funk M (1994) Regulatable promoters of Saccharomyces cerevisiae: comparison of transcriptional activity and their use for heterologous expression. Nucleic Acids Res **22**: 5767–5768

Nakamura RL, McKendree WL, Hirsch RE, Sedbrook JC, Gaber RF, Sussman MR (1995) Expression of an Arabidopsis potassium channel gene in guard cells. Plant Physiol **109**: 371–374

Navarrete C, Petrezselyova S, Barreto L, Martinez JL, Zahradka J, Arino J, Sychrova H, Ramos J (2010) Lack of main K plus uptake systems in Saccharomyces cerevisiae cells affects yeast performance in both potassium-sufficient and potassium-limiting conditions. FEMS Yeast Res **10**: 508–517

Obrdlik P, El-Bakkoury M, Hamacher T, Cappellaro C, Vilarino C, Fleischer C, Ellerbrok H, Kamuzinzi R, Ledent V, Blaudez D, et al (2004) K+ channel interactions detected by a genetic system optimized for systematic studies of membrane protein interactions. Proc Natl Acad Sci **101**: 12242–7

Pardo JM, Quintero FJ (2002) Plants and sodium ions: keeping company with the enemy. Genome Biol **3**: doi:10.1186/gb-2002-3-6-reviews1017

Paumi CM, Menendez J, Arnoldo A, Engels K, Iyer KR, Thaminy S, Georgiev O, Barral Y, Michaelis S, Stagljar I (2007) Mapping protein-protein interactions for the yeast ABC transporter Ycf1p by integrated split-ubiquitin membrane yeast two-hybrid analysis. Mol Cell **26**: 15–25

Pilot G, Pratelli R, Gaymard F, Meyer Y, Sentenac H (2003) Five-group distribution of the Shaker-like K+ channel family in higher plants. J Mol Evol **56**: 418–434

Planes MD, Niñoles R, Rubio L, Bissoli G, Bueso E, García-Sánchez MJ, Alejandro S, Gonzalez-Guzmán M, Hedrich R, Rodriguez PL, et al (2015) A mechanism of growth inhibition by abscisic acid in germinating seeds of Arabidopsis thaliana based on inhibition of plasma membrane H+-ATPase and decreased cytosolic pH, K+, and anions. J Exp Bot **66**: 813–825

Prokhnevsky AI, Peremyslov V V., Dolja V V. (2005) Actin Cytoskeleton Is Involved in Targeting of a Viral Hsp70 Homolog to the Cell Periphery. J Virol **79**: 14421–14428

Rodríguez-Navarro A (2000) Potassium transport in fungi and plants. Biochim Biophys Acta **1469**: 1–30

Ronzier E, Corratgé-Faillie C, Sanchez F, Prado K, Brière C, Leonhardt N, Thibaud JB, Xiong TC (2014) CPK13, a noncanonical Ca2+-dependent protein kinase, specifically inhibits KAT2 and KAT1 shaker K+ channels and reduces stomatal opening. Plant Physiol **166**: 314–326

Saponaro A, Porro A, Chaves-Sanjuan A, Nardini M, Rauh O, Thiel G, Moroni A (2017) Fusicoccin Activates KAT1 Channels by Stabilizing Their Interaction with 14-3-3 Proteins. Plant Cell **29**: 2570–2580

Sarrion-Perdigones A, Vazquez-Vilar M, Palací J, Castelijns B, Forment J, Ziarsolo P, Blanca J, Granell A, Orzaez D (2013) GoldenBraid 2.0: a comprehensive DNA assembly framework for plant synthetic biology. Plant Physiol **162**: 1618–1631

Sato A, Sato Y, Fukao Y, Fujiwara M, Umezawa T, Shinozaki K, Hibi T, Taniguchi M, Miyake H, Goto DB, et al (2009) Threonine at position 306 of the KAT1 potassium channel is essential for channel activity and is a target site for ABA-activated SnRK2/OST1/SnRK2.6 protein kinase. Biochem J **424**: 439–448

Schachtman DP, Schroeder JI, Lucas WJ, Anderson JA, Gaber RF (1992) Expression of an inward-rectifying potassium channel by the Arabidopsis KAT1 cDNA. Science (80-) **258**: 1654–1658

Sessions A, Burke E, Presting G, Aux G, McElver J, Patton D, Dietrich B, Ho P, Bacwaden J, Ko C, et al (2002) A high-throughput Arabidopsis reverse genetics system. Plant Cell **14**: 2985–2994

Sieben C, Mikosch M, Brandizzi F, Homann U (2008) Interaction of the K(+)-channel KAT1 with the coat protein complex II coat component Sec24 depends on a di-acidic endoplasmic reticulum export motif. Plant J **56**: 997–1006

Sottocornola B, Gazzarrini S, Olivari C, Romani G, Valbuzzi P, Thiel G, Moroni A (2008) 14-3-3 proteins regulate the potassium channel KAT1 by dual modes. Plant Biol **10**: 231–236

Sottocornola B, Visconti S, Orsi S, Gazzarrini S, Giacometti S, Olivari C, Camoni L, Aducci P, Marra M, Abenavoli A, et al (2006) The potassium channel KAT1 is activated by plant and animal 14-3-3 proteins. J Biol Chem **281**: 35735–35741

Sutter JU, Campanoni P, Tyrrell M, Blatt MR (2006) Selective mobility and sensitivity to SNAREs is exhibited by the Arabidopsis KAT1 K+ channel at the plasma membrane. Plant Cell **18**: 935–954

Sutter JU, Sieben C, Hartel A, Eisenach C, Thiel G, Blatt MR (2007) Abscisic acid triggers the endocytosis of the arabidopsis KAT1 K+ channel and its recycling to the plasma membrane. Curr Biol **17**: 1396–1402

Szyroki A, Ivashikina N, Dietrich P, Roelfsema MR, Ache P, Reintanz B, Deeken R, Godde M, Felle H, Steinmeyer R, et al (2001) KAT1 is not essential for stomatal opening. Proc Natl Acad Sci U S A **98**: 2917–2921

Takayama S, Reed JC (2001) Molecular chaperone targeting and regulation by BAG family proteins. Nat Cell Biol **3**: doi:10.1038/ncb1001-e237

Véry AA, Gaymard F, Bosseux C, Sentenac H, Thibaud JB (1995) Expression of a cloned plant K+ channel in Xenopus oocytes: analysis of macroscopic currents. Plant J **7**: 321–332

Véry AA, Sentenac H (2003) Molecular mechanisms and regulation of K+ transport in higher plants. Annu Rev Plant Biol **54**: 575–603

Wang Y, Hills A, Blatt MR (2014) Systems analysis of guard cell membrane transport for enhanced stomatal dynamics and water use efficiency. Plant Physiol **164**: 1593–1599

Wang Y, Holroyd G, Hetherington AM, Ng CKY (2004) Seeing “cool” and “hot” - Infrared thermography as a tool for non-invasive, high-throughput screening of Arabidopsis guard cell signalling mutants. J Exp Bot **55**: 1187–1193

Williams B, Kabbage M, Britt R, Dickman MB (2010) AtBAG7, an Arabidopsis Bcl-2-associated athanogene, resides in the endoplasmic reticulum and is involved in the unfolded protein response. Proc Natl Acad Sci **107**: 6088–6093

Winter D, Vinegar B, Nahal H, Ammar R, Wilson G V, Provart NJ (2007) An "Electronic Fluorescent Pictograph" browser for exploring and analyzing large-scale biological data sets. PLoS One **2**: e718

Wu HY, Liu KH, Wang YC, Wu JF, Chiu WL, Chen CY, Wu SH, Sheen J, Lai EM (2014) AGROBEST: an efficient Agrobacterium-mediated transient expression method for versatile gene function analyses in Arabidopsis seedlings. Plant Methods **10**: 19

Xicluna J, Lacombe B, Dreyer I, Alcon C, Jeanguenin L, Sentenac H, Thibaud JB, Chérel I (2007) Increased functional diversity of plant K+ channels by preferential heteromerization of the shaker-like subunits AKT2 and KAT2. J Biol Chem **282**: 486–494

Yan A, Wu E, Lennarz WJ (2005) Studies of yeast oligosaccharyl transferase subunits using the split-ubiquitin system: topological features and in vivo interactions. Proc Natl Acad Sci U S A **102**: 7121–7126

Yang Y, Costa A, Leonhardt N, Siegel RS, Schroeder JI (2008) Isolation of a strong Arabidopsis guard cell promoter and its potential as a research tool. Plant Methods **4**: 6

Young JC (2014) The role of the cytosolic HSP70 chaperone system in diseases caused by misfolding and aberrant trafficking of ion channels. Dis Model Mech **7**: 319–329

Zhang B, Karnik R, Waghmare S, Donald N, Blatt MR (2017) VAMP721 Conformations Unmask an Extended Motif for K+ Channel Binding and Gating Control. Plant Physiol **173**: 536–551

Zhang B, Karnik R, Wang Y, Wallmeroth N, Blatt MR, Grefen C (2015) The Arabidopsis R-SNARE VAMP721 Interacts with KAT1 and KC1 K+ Channels to Moderate K+ Current at the Plasma Membrane. Plant Cell **27**: 1697–1717

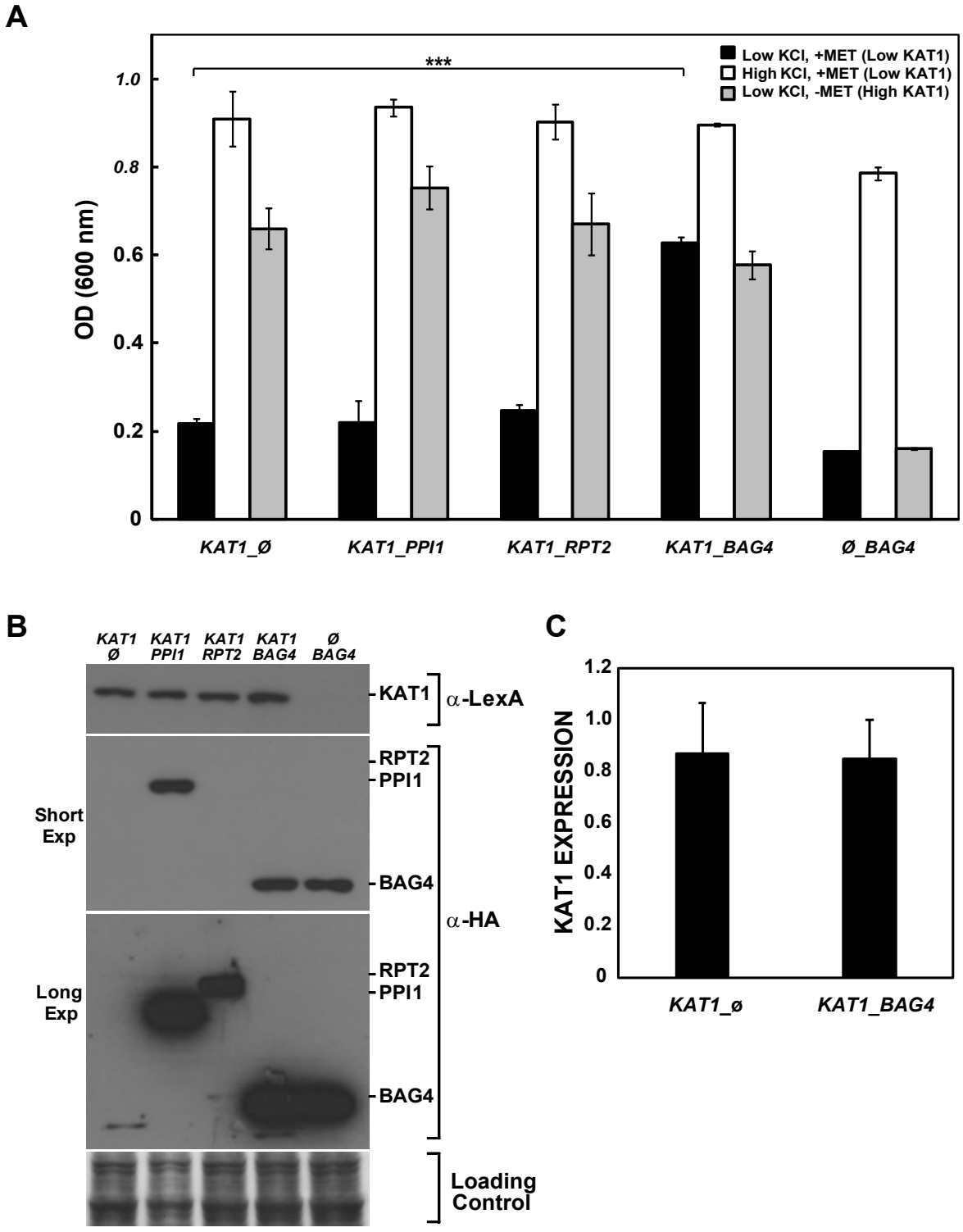

Figure 1. Effect of the co-expression of interacting proteins on the functional complementation by KAT1 in yeast. A) The indicated plasmids were co-transformed in the trk1 trk2 mutant strain (PLY240) and the growth of the strains was assayed as described in Materials and Methods using the Translucent media (which contains 12 µM potassium) with or without methionine supplementation to decrease the expression of KAT1 (under c ontrol of the MET25 promoter). The graph shows the average value of the optical density at 72 hours for triplicate determinations and the experiment was done with at least 3 independent transformants for each plasmid combination. (Translucent media with no KCl supplementation = Low KCl (12 µM K+); Translucent media containing 0.75 mg/mL methionine = Low KAT1; Translucent media + 50 mM KCl added = High KCl; Translucent media -/+ KCl without methionine = High KAT1). B) Immunoblot analysis of protein extracts from the indicated strains showing the correct expression of each of the fusion proteins. The KAT1 bait vector protein is detected with the anti-LexA antibody and the prey proteins with the anti-HA antibody. Results for a representative clone are shown. The long exposure is included to visualize the expression of the RPT2 prey protein, which accumulates less than the other two prey proteins. Data presented are the mean ±SD and similar results were observed for three independent transformants. Asterisks (**) indicate statistical significance (Student t test) with a p value < 0.01. C) The KAT1 signal and the corresponding loading control were quantified using the ImageJ software and the average values of KAT1/loading control (Normalized KAT1) was calculated for 6 control strains (KAT1_empty vector) and 7 KAT1_BAG4 strains. Data presented are the mean ±SD.

Figure 1

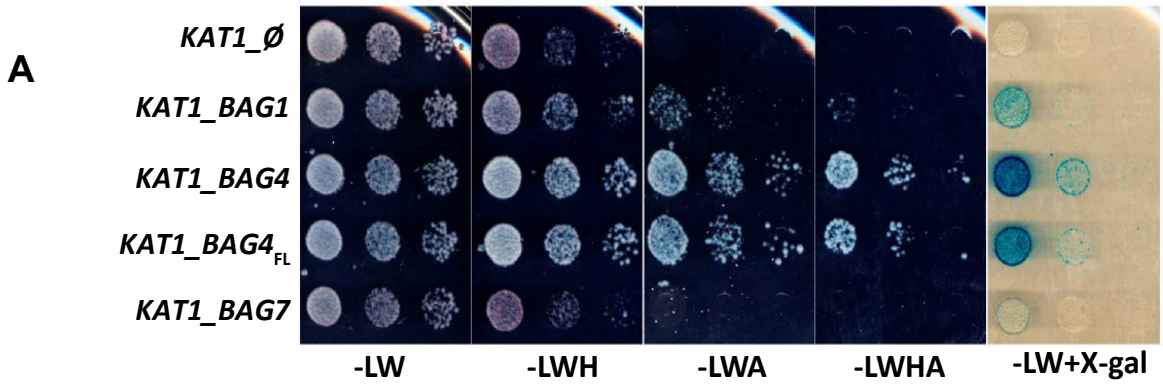

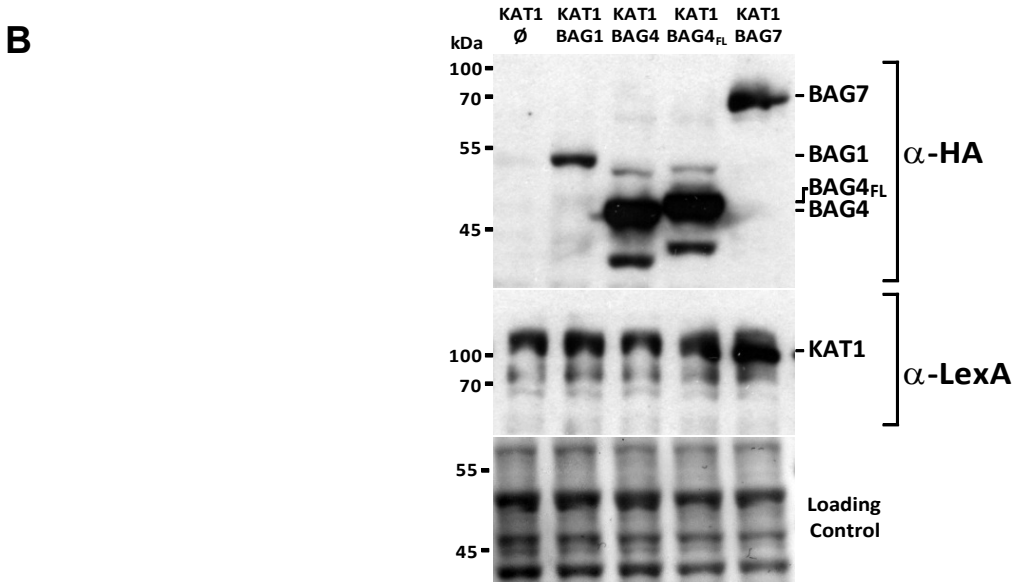

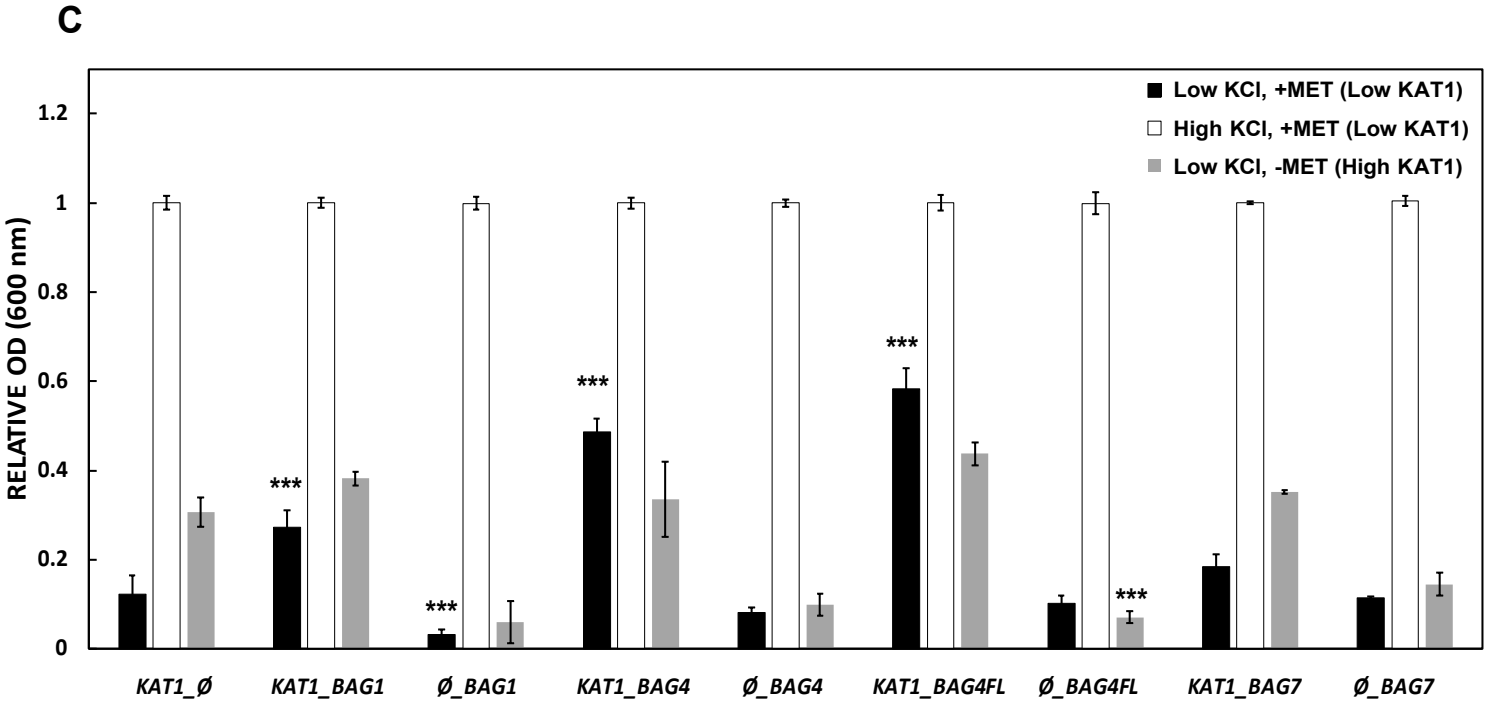

Figure 2. Study of the specificity of the interaction between KAT1 and other BAG family members. A) The indicated plasmids were transformed into the THY.AP4 strain and grown to saturation in selective media. Serial dilutions were spotted onto media with the indicated composition to test for the protein-protein interaction between KAT1 and the indicated BAG family proteins. Identical results were observed for four independent clones. B) Immunoblot analysis of protein extracts from the indicated strains showing the correct expression of each of the fusion proteins. The KAT1 bait protein is detected with the anti-LexA antibody and the prey proteins with the anti-HA antibody. Results for a representative clone are shown. C) The indicated plasmids were co-transformed in the *trk1 trk2* mutant strain (PLY240) and the growth of the strains was assayed as described in Figure 1A. The average value of triplicate determinations of the optical density of the growth normalized to the potassium supplemented media is shown for each strain. Similar results were observed for 3 independent clones of each plasmid combination. Asterisks (***) indicate statistical significance (Student t test) with a p value < 0.001 compared to the *KAT1_Ø* strain.

Figure 2

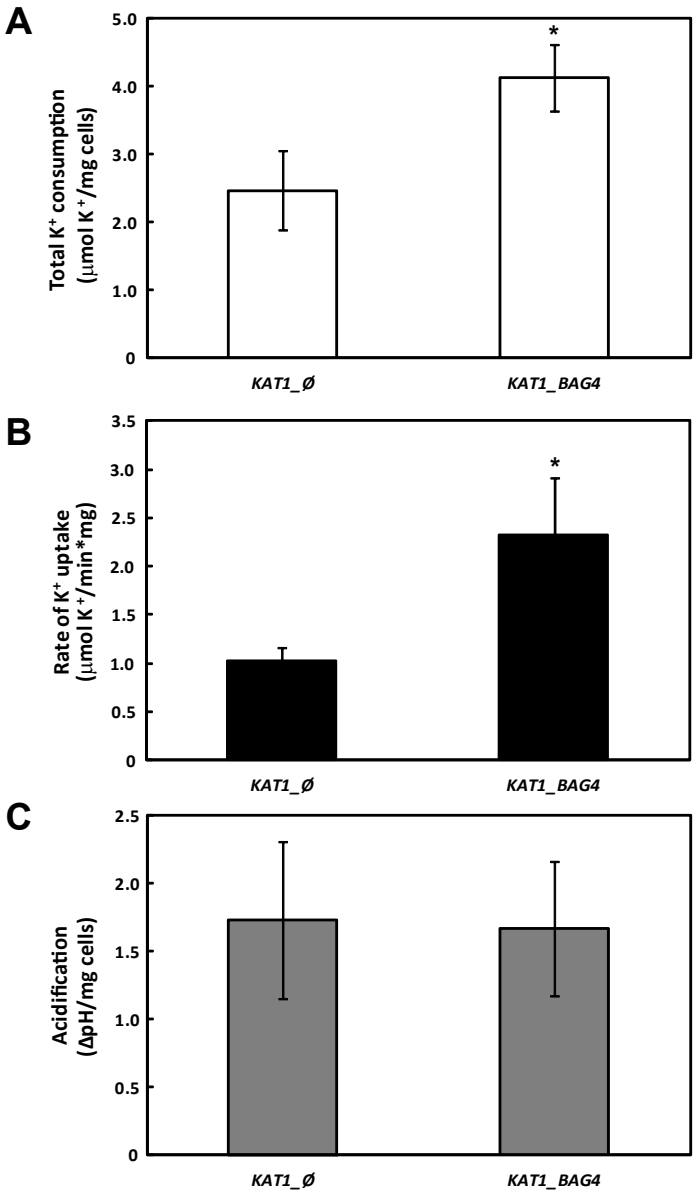

Figure 3. Potassium uptake and external acidification. The indicated plasmids were co-transformed in the *trk1 trk2* mutant strain (PLY240) and the strains were grown in low KCl and low KAT1 conditions and processed as described in Materials and Methods. A) The bars represent the average value for three independent experiments for the total potassium uptake for 45 minutes expressed as µmol K+/mg cells. B) The bars represent the average value for three independent experiments for the rate of potassium uptake expressed as µmol K+/min*mg cells calculated using the slope of the depletion curve normalized to the wet weight of the cells. C) The bars represent the average value for three independent experiments of the change in the pH value measured in parallel with the potassium consumption. The change in the external pH was determined during the first 15 minutes after glucose addition and was normalized to the wet weight of the cells. Asterisks (*) indicate statistical significance (Student t test) with a p value < 0.05.

Figure 3

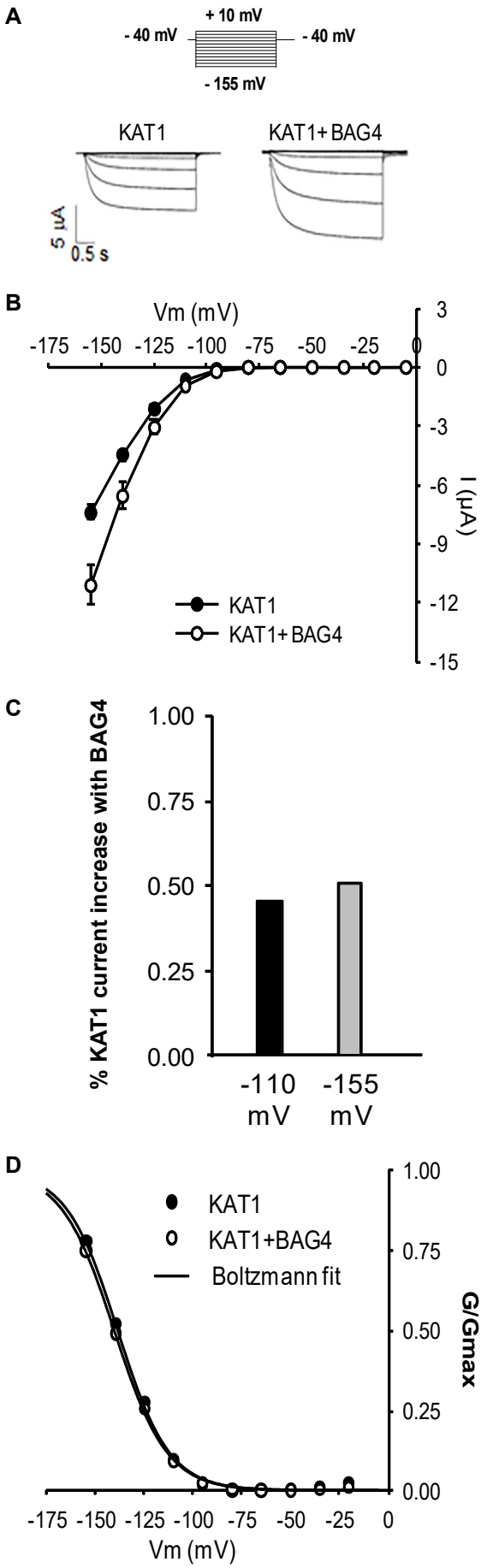

Figure 4. BAG4 co-expression increases KAT1 current in Xenopus oocytes. A) Voltage-clamp protocol and representative current traces recorded by two-electrode voltage clamp in the presence of 100 mM KCl on oocytes co-expressing KAT1 or KAT1 and BAG4. B) KAT1 current (I) –voltage (V) relationships of oocytes co-expressing KAT1 and BAG4 (white circles) or expressing KAT1 alone (black circles). Data are means +/- SE (n=7 for KAT1, n=11 for KAT1 + BAG4), and are representative of two experiments performed on different oocyte batches. C) Increase of mean KAT1 current upon BAG4 co-expression, at -110 mV (black) and at -155 mV (grey). D) Voltage-dependence of KAT1-current activation in the presence of BAG4 (white circles) or with KAT1 expressed alone (black circles). Gating parameters (z, gating charge, and Ea50, half-activation potential) were estimated by performing fits to the KAT1 I-V relationships (in the presence or absence of BAG4) with a Boltzmann function coupled to a linear relation (Lebaudy et al., 2010).

Figure 4

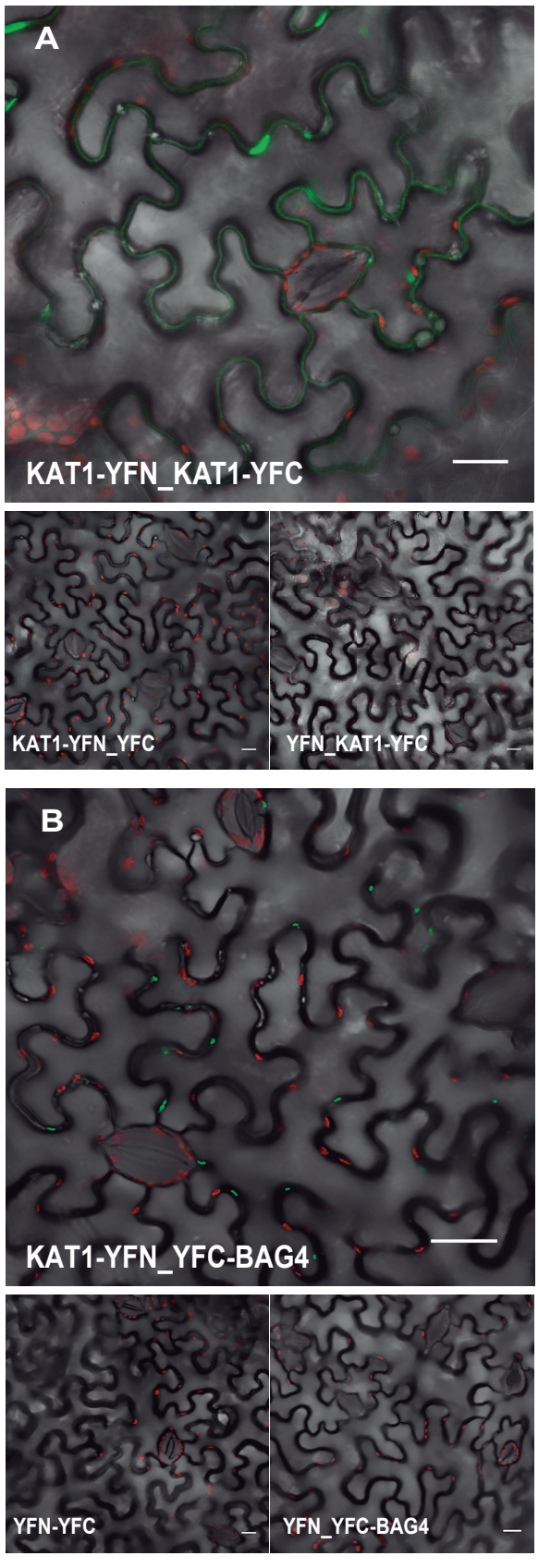
A
KAT1-YFN_KAT1-YFC
KAT1-YFN_YFC
YFN_KAT1-YFC
B
KAT1-YFN_YFC-BAG4
YFN-YFC
YFN_YFC-BAG4
C
35S:KAT1-YFP
35S:myc-BAG4
35S:myc-BAG4
IP FT Input IP FT Input
36kDa
α-myc
106kDa
α-GFP

Figure 5

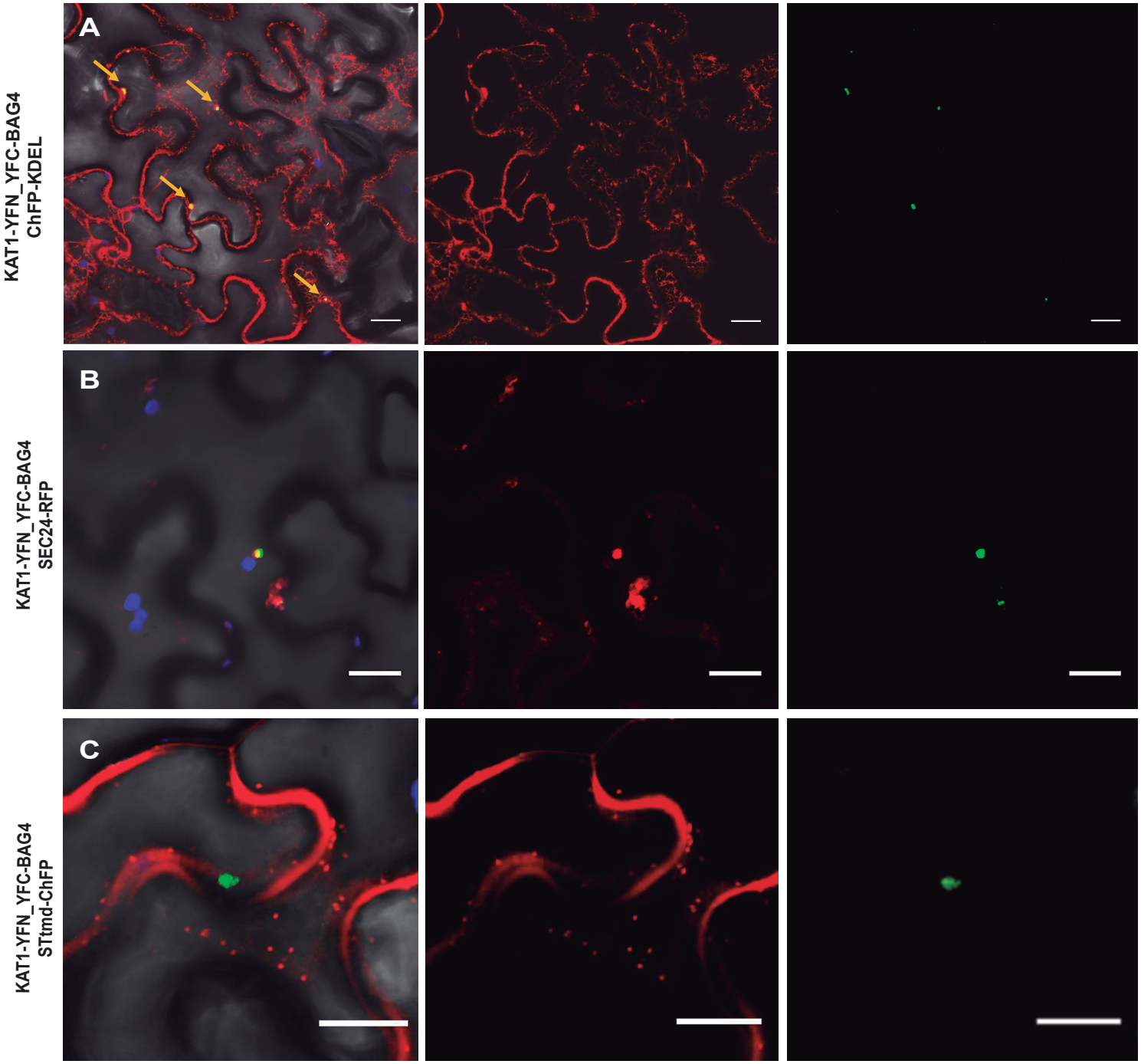
A
KAT1-YFN_YFC-BAG4
ChFP-KDEL
B
KAT1-YFN_YFC-BAG4
SEC24-RFP
C
KAT1-YFN_YFC-BAG4
STtmd-ChFP

Figure 6

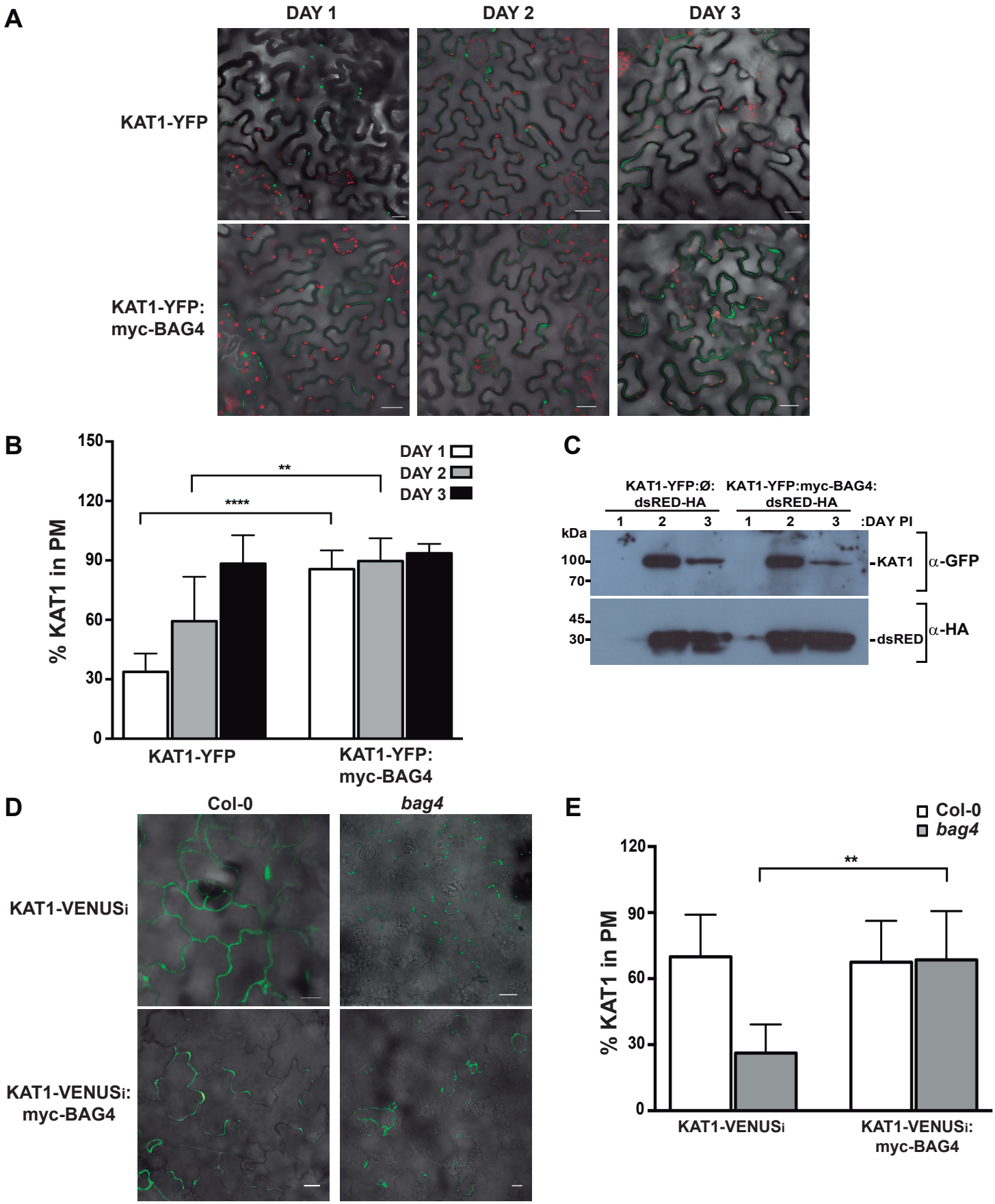

Figure 7. BAG4 expression effects the subcellular localization of KAT1. A) Plasmids containing KAT1-YFP or both KAT1-YFP and BAG4 were transiently expressed in *N. benthamiana* using agro-infiltration. The fluorescence signal was analysed by confocal microscopy days 1, 2 and 3 days post-infiltration. Representative images are shown. Similar results were observed in three independent experiments. B) The percentage of the fluorescence signal present in the plasma membrane was quantified using ImageJ, as described in Materials and Methods. The graph shows the average values ±SD for 10 cells for each condition tested. C) Similar experiments as described in part a) were performed, but using GoldenBraid plasmids containing KAT1-YFP:dsRED-HA or KAT1-YFP:myc-BAG4:dsRED-HA. Whole cell extracts were prepared from infiltrated areas (previously confirmed to express KAT1-YFP) and proteins were processed for immunodetection. The dsRED-HA protein serves as an internal control for the efficiency of transient expression. D) The KAT1-VENUSintron (KAT1-VENUSi, top row) or the KAT1-VENUSintron_BAG4 (bottom row) plasmids were transiently expressed in the Col-0 and the bag4 mutant Arabidopsis lines using agro-infiltration. The fluorescence signal was analyzed by confocal microscopy 2 days after infiltration. Representative images are shown and similar results were observed in three independent experiments. (Bar = 20μm) E) The percentage of the fluorescence signal present in the plasma membrane was quantified using ImageJ, as described in Materials and Methods. The graph shows the average values ±SD for 10 cells for each condition tested.

Figure 7

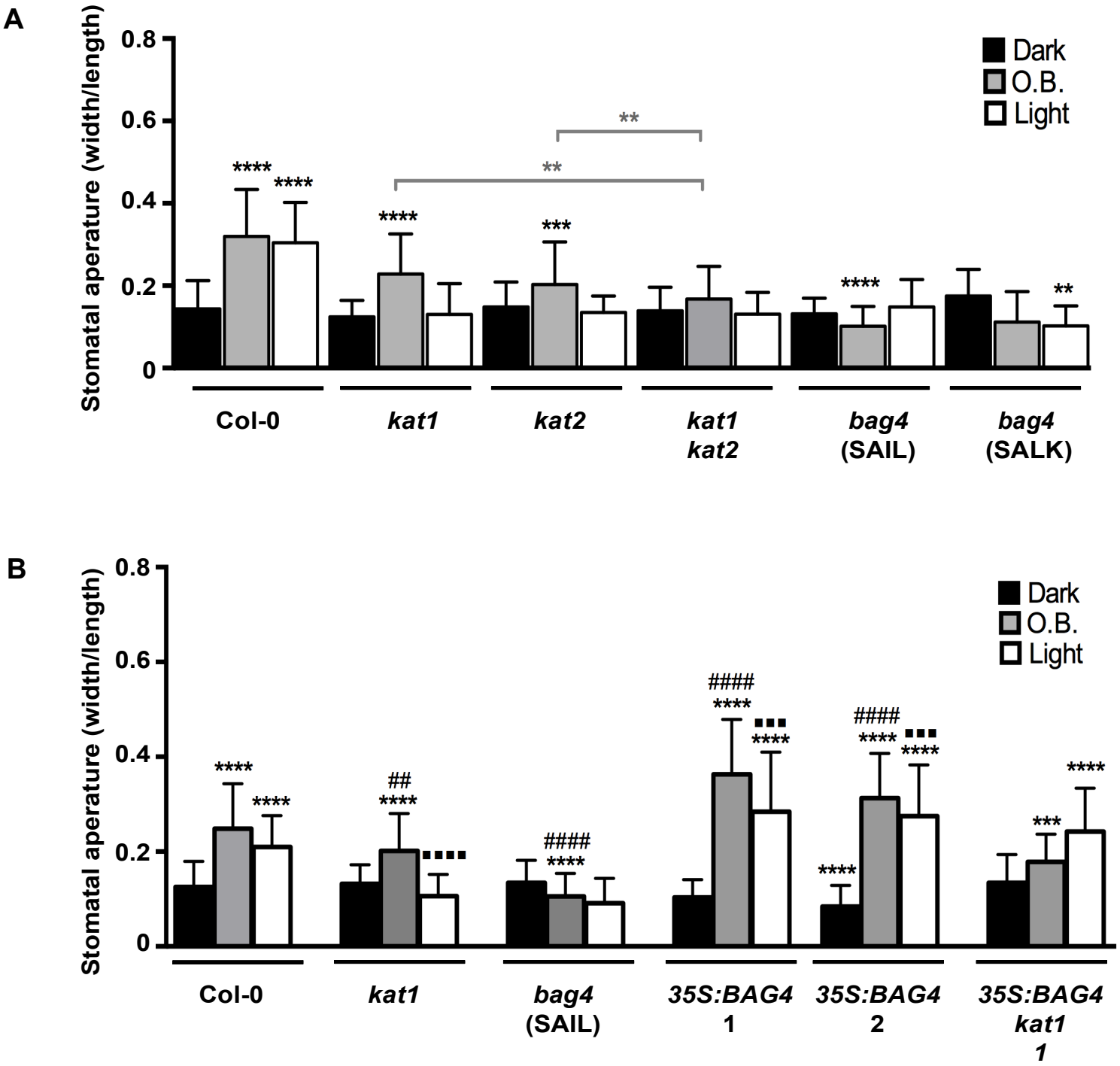

Figure 8. Effect of BAG4 loss and gain-of-function on stomatal aperture. Stomata from the indicated Arabidopsis lines were analyzed as described in Materials and Methods. The data show the average ratio for 60-100 stomata and the error bars represent the standard deviation. A) The width/length ratio of stomata of the different mutant lines were determined in leaves from the indicated lines harvested 1 hour before the lights turned on (Dark), incubated for 2.5 hours in opening buffer in the dark (Opening buffer, O.B.) or 2.5 hours after the lights turned on (Light). Similar results were observed in three independent experiments. B) The width/length ratio of stomata of control lines and Col-0 and kat1 homozygous for 35S:BAG4 transgene were determined as described in A. For both experiments, the asterisks indicate statistical significance as compared to the Col-0 dark control (Student t test) (**: p value <0.01; ***: p value < 0.001; **** p value < 0.0001). The length/width ratio was also significantly increased in BAG4 overexpressing lines in both light and opening buffer (# indicates statistical comparison with Col-0 O.B. and ▪ indicates statistical comparison with Col-0 light).

Figure 8

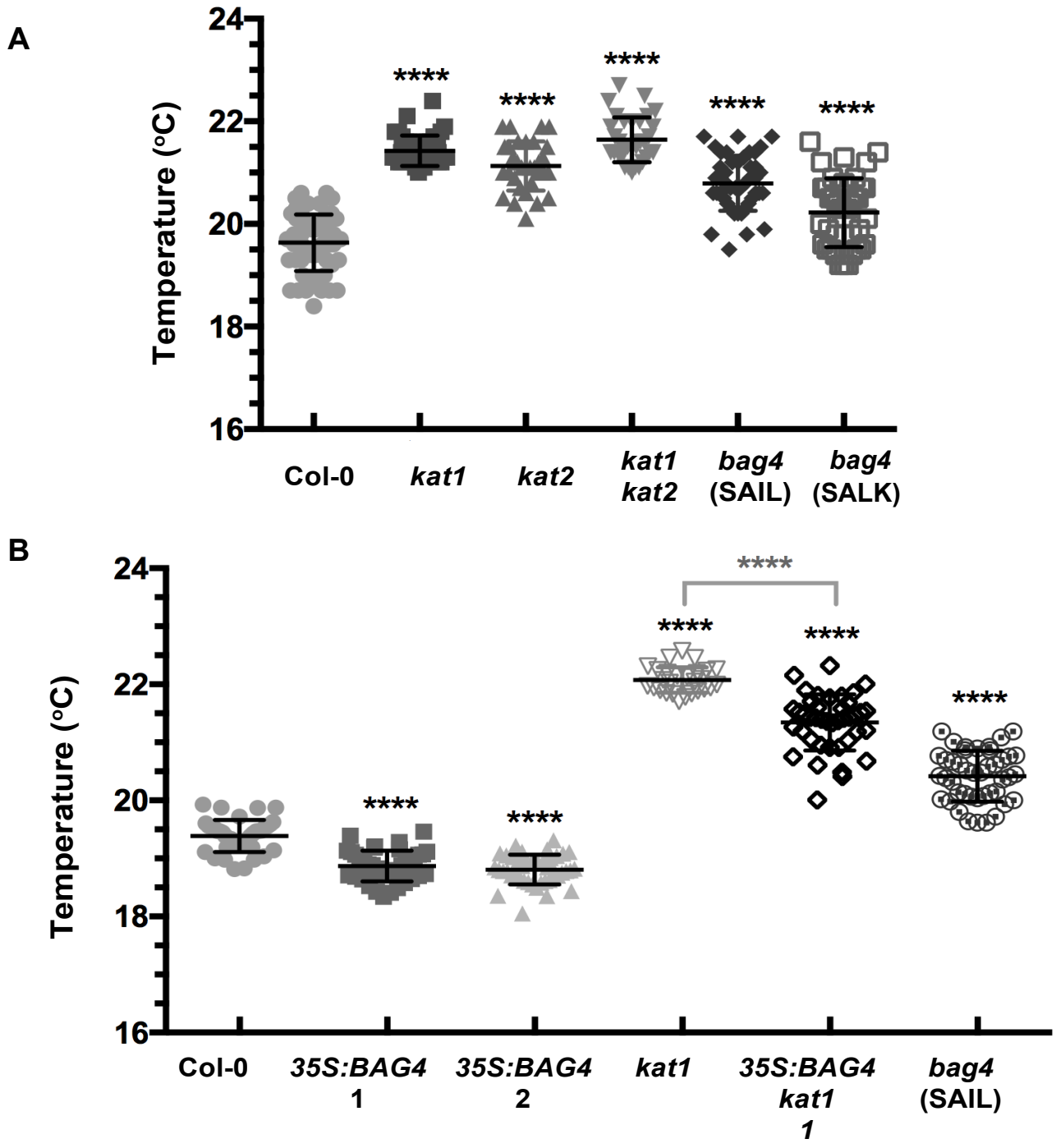

Figure 9. Effect of BAG4 loss and gain-of-function on leaf temperature. The same lines described in Figure 7 were analyzed for leaf temperature using an infrared thermography, as described in Materials and Methods (Panel A mutant lines, Panel B control and 35S:BAG4 lines). Each symbol represents an indifvidual measurment and the bar represents the average value for 10 measurements of 6 different plants for each genotype. The error bars represent the standard deviation. For both experiments, the asterisks indicate statistical significance as compared to the Col-0 control or the comparisons indicated by the brackets above the graphs (Student t-test) (: p value <0.01; ***: p value < 0.001; **** p value < 0.0001).**

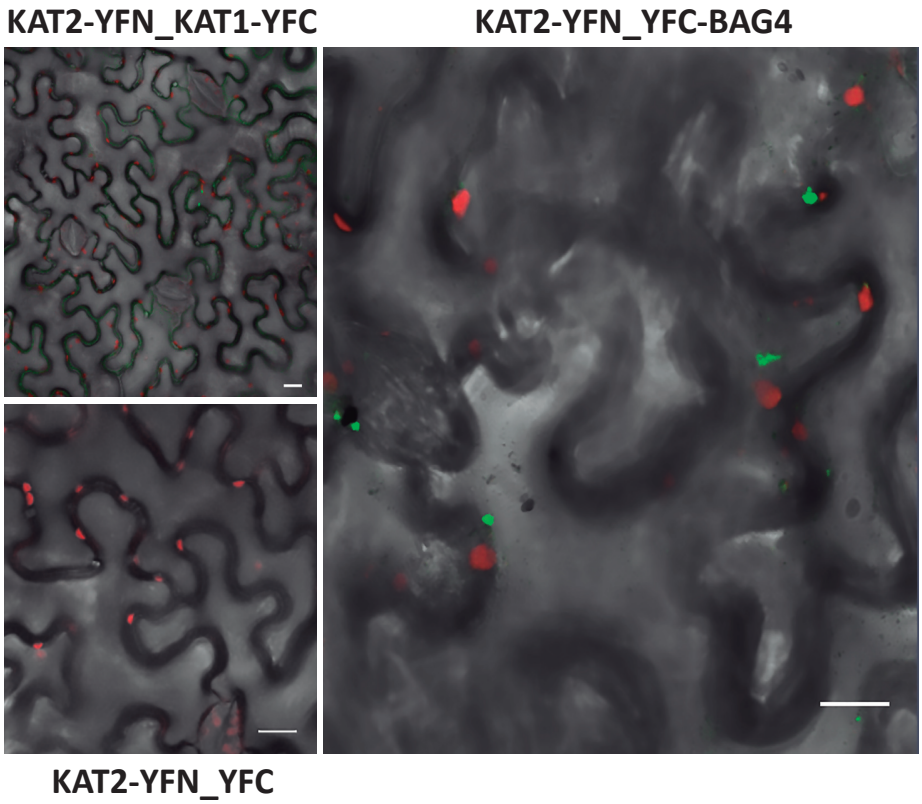

Figure 10. BAG4 interacts with KAT2 in BiFC assays in *N. benthamiana*. Interaction assays were carried out and analyzed as described in the legend to Figure 5. As shown, a similar pattern of interaction is observed for KAT2 when tested with BAG4 (compare with Figure 5B). In this image, the BiFC signals corresponding to the KAT2-KAT1 and KAT2-BAG4 interactions are shown in green and the chloroplast autofluorescence is shown in red. (Bar = 20μm)

Figure 10

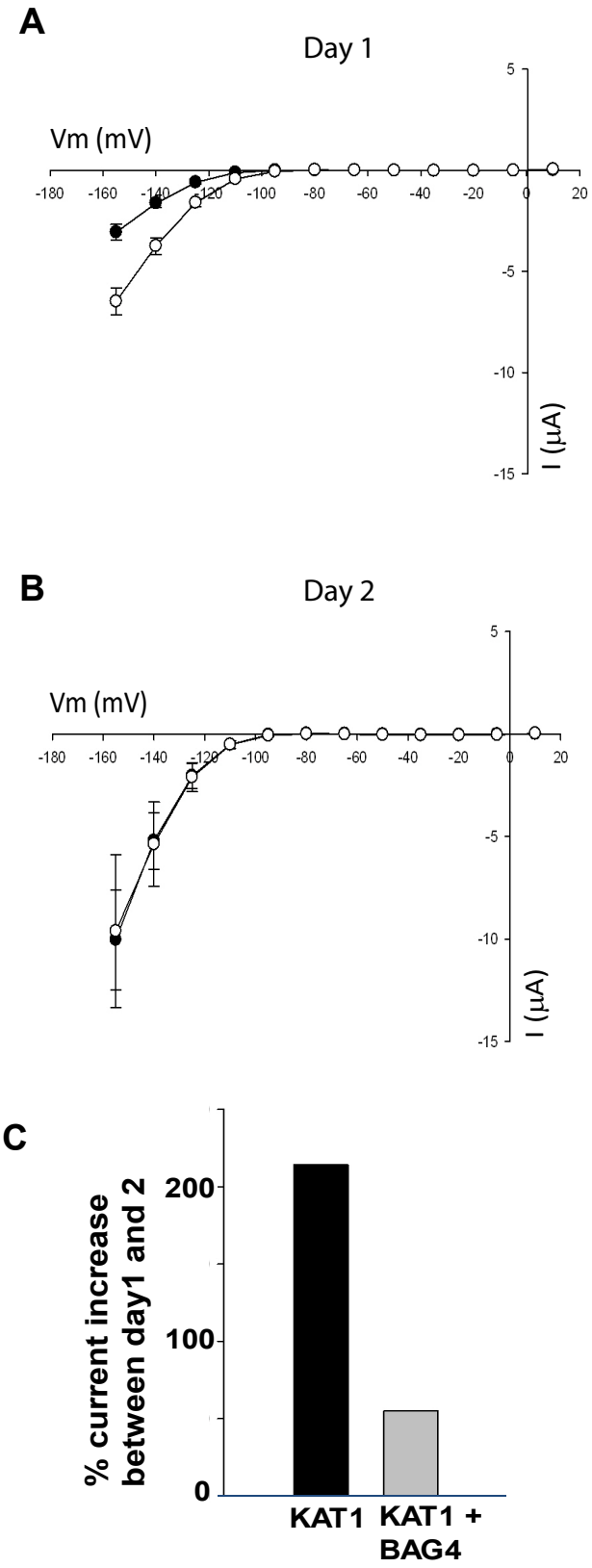

Supplemental Figure S1. BAG4 co-expression favors early activity of KAT1 in Xenopus oocytes. A-B) KAT1 current (I) –voltage (V) relationships of oocytes co-expressing KAT1 and BAG4 (white circles) or expressing KAT1 alone (black circles) one day (A) or two days after RNA injection (B). Oocytes were injected with 30 ng of KAT1 cRNA or co-injected with 30 ng of KAT1 cRNA and 22.5 ng of BAG4 cRNA and currents were recorded by two-electrode voltage clamp in the presence of 100 mM KCl. Data are means +/- SE (n=8 in A, 5 in B for KAT1, n=12 in A, 5 in B for KAT1 + BAG4). C) Increase of mean current between Day 1 and Day 2 at -155 mV in oocytes expressing KAT1 alone (black) or co-expressing KAT1 and BAG4 (grey).

Figure S1

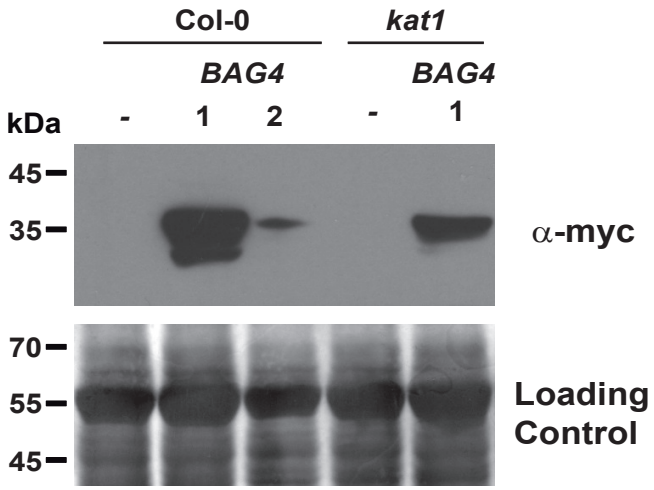

Supplemental Figure S2. Immunodetection of myc-BAG4 protein in homozygous transgenic lines. Whole cell extracts from the same lines used in Figures 7 and 8 were prepared from the indicated control or 35S:myc-BAG4 lines and proteins were processed for immunodetection. 100 mg of leaves from 5-week-old plants grown under short day conditions were harvested just before the lights turned on and then frozen, ground with glass beads and resuspended in 250 μL of Laemmli 2x. After 5 min incubation on ice, 20 μL of the supernatant were loaded on the gel and processed for immunoblotting.

Figure S2